CHAPTER 6

SYNTHESIS AND CRYSTAL STRUCTURES OF NEW LANTHANIDE FRAMEWORKS WITH A FLEXIBLE POLYCARBOXYLATE LIGAND

Lanthanide metal–organic hybrid materials are currently of great interest, not only because of the inherent diversity of their solid state chemistry but also for their potential applications as described in Chapter 1 [1–3]. Accounting for these applications, luminescence property is widely acknowledged as the major merit of the lanthanide metals. However, only the lanthanides in the framework, they cannot exhibit the distinguished luminescence behavior. This can be accomplished by the use of organic ligands as an antenna assisting in energy absorption and subsequent transfer process to the lanthanides in the complexes [4, 5]. Previous literature study shows that polycarboxylate ligands display a good antenna effect with respect to the lanthanide ions [6, 7]. Moreover the polycarboxylato groups of these flexible multipodal ligands can assume various conformations and coordination patterns resulting in the versatile unusual hybrid networks and therefore properties. Some flexible triazine–based derivative ligands such as *N*,*N*′,*N*′′–1,3,5–triazine–2,4,6–triyltris–glycine (TTG) [8], 2,2′,2′′–[1,3,5–triazine–2,4,6–triyltris(thio)]tris–acetic acid (TTTA) [9], and 1,3,5–

triazine–2,4,6–triamine hexaacetic acid (TTHA) [10] were formerly reported in the fabrication of various types of network structures. With reference to the TTHA, there are twenty–six structures reported in Cambridge Structure Database during 2000 to 2012 [11]. Among these structures, the coordinating metals are mostly the transition and alkali metals except for a series of $[Ln_2(TTHA)(H_2O)_4]\cdot 9H_2O$ where Ln = Eu, Tb, Gd and Dy) [12]. Moreover, the various types of coordination modes of the carboxylato group in TTHA ligand are also considered as depicted in Figure 6.1 [11].

In this chapter we reported the synthesis of four new distinct structures of the lanthanide frameworks using TTHA as a flexible multipodal linker *i.e.*, $Ln_4(C_{15}H_{12}O_{12}N_6)_2(C_8H_9N_2O_6)_{0.5}(H_2O)_3\cdot 5H_2O$ where Ln = Pr^{III} (**IXa**) and Nd^{III} (**IXb**), $Sm_8(C_{15}H_{12}O_{12}N_6)_4(C_8H_9N_2O_6)_{0.5}(H_2O)_8\cdot 4H_2O$ (**X**), $Ln_4(C_{15}H_{13}O_{12}N_6)_2(SO_4)(H_2O)_4 .2H_2O$ where Ln = Pr (**XIa**) and Nd (**XIb**), and $Sm_2(C_{15}H_{12}O_{12}N_6)(H_2O)_4.9H_2O$ **(XII).** Within the reported structures, the framework structure of **XII** is isostructure to the previously reported lanthanide–TTHA series [12]. In addition, *in situ* synthesis of 2,5–dioxo–piperazine–1,4–diacetic acid found in compound **IXa**, **IXb** and **X** is presented.

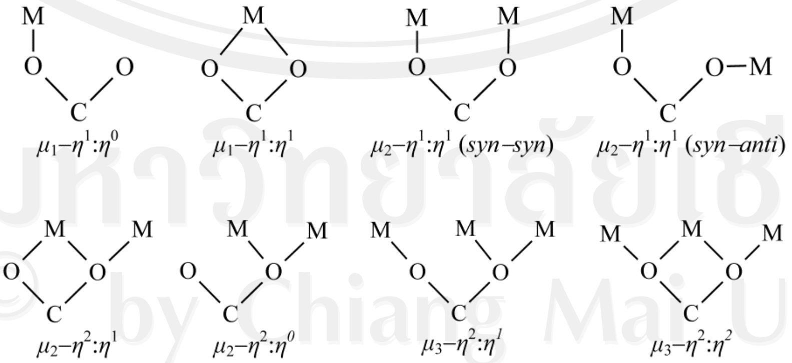

Figure 6.1 Diagrams showing different coordination modes of the carboxylato anions reported to the Cambridge Structure Database.

6.1 Experimental

6.1.1 Synthesis and crystal growth

The starting materials $Ln_2(SO_4)_3.8H_2O$ where Ln = Pr, Nd and Sm, were prepared by dissolving Pr_6O_{11} (TJTM, 99%), Nd_2O_3 (TJTM, 99%) and Sm_2O_3 (TJTM, 99%) accordingly in diluted aqueous solution of H_2SO_4 (Merck, 98%). The solutions were left undisturbed at 80 °C to let the $Pr_2(SO_4)_3.8H_2O$, $Nd_2(SO_4)_3.8H_2O$ and $Sm_2(SO_4)_3.8H_2O$ crystals to slowly crystallize after few days. The TTHA ligand was synthesized by the microwave method following the procedure reported by W. Karuehanon *et.al*. [13].

The crystal products of $Ln_4(C_{15}H_{12}O_{12}N_6)_2(C_8H_{10}O_6N_2)_{0.5}(H_2O)_3.5H_2O$ (Ln = Pr **(IXa)** and Nd (**IXb)**) were synthesized and growth from the hydrothermal reaction of an aqueous mixture of $Ln_2(SO_4)_3.8H_2O$ (Ln = Pr and Nd; 0.30 mmol) and $C_{15}H_{18}N_6O_{12}$ (H_6TTHA; 1,3,5–triazine–2,4,6–triamine hexaacetic acid; 0.50 mmol) in 10.00 cm^3 of deionized water. The reaction was performed under an autogenous pressure generated at 180 °C for 3 days. The final products are green block **(IXa**) and purple block (**IXb**) crystals. The similar synthetic procedure and chemical stoichiometry as summarized in Table 6.1 were adopted for the synthesis of $Sm_8(C_{15}H_{12}O_{12}N_6)_4(C_8H_8O_6N_2)_{0.5}(H_2O)_8.4H_2O$ **(X)**, $Ln_4(C_{15}H_{13}O_{12}N_6)_2(SO_4)(H_2O)_4.2H_2O$ (Ln = Pr (**XIa**) and Nd (**XIb**)) and $Sm_2(C_{15}H_{12}O_{12}N_6)(H_2O)_4.9H_2O$ **(XII).**

Elemental compositions of the yielded crystals were determined by elemental analysis: (**IXa**) *Calc.* C, 23.42; H, 2.18; N, 10.44; *Found.* C, 19.38; H, 2.43; N, 9.07;
(**X**) *Calc.* C, 22.70; H, 1.77; N, 10.35; *Found.* C, 22.54; H, 2.64; N, 10.14;
(**XIa**) *Calc.* C, 21.20; H, 2.00; N, 9.89; *Found.* C, 20.39; H, 2.47; N, 9.53;
(**XII**) *Calc.* C, 18.42; H, 3.07; N, 8.60; *Found.* C, 19.03; H, 3.56; N, 8.65.

The FT–IR spectra were collected on also the ground crystals prepared as a KBr pellet (BDH, 98.5%) within the 4000–400 cm^{-1} region and a resolution of 0.5 cm^{-1}, using Bruker Tensor 27 FT–IR spectrometer. Thermal stability was investigated by thermogravimetric analysis (TGA) which was conducted on NETZSCH STA 409 PC/PG instrument under a flow of N_2 gas in a temperature range between 20 °C and 1200 °C using a heating rate of 10 $°Cmin^{-1}$. A UV–Vis spectra were collected in a range of 200–800 nm on a suspension of the ground crystals in water using Perkin Elmer UV LAMDA 25 spectrophotometer.

Table 6.1 Synthetic conditions employed for the synthesis of **IXa**, **IXb**, **X**, **XIa**, **XIb** and **XII.**

Product codes	Synthetic conditions	Temp (°C)	Time (h)	Crystal appearance
IXa	(0.30mmol) $Pr_2(SO_4)_3.8H_2O$ + (0.50mmol) H_6TTHA + (556mmol) H_2O	180	72	green block
IXb	(0.30mmol) $Nd_2(SO_4)_3.8H_2O$ + (0.50mmol) H_6TTHA + (556mmol) H_2O	180	72	purple block
X	(0.30mmol) $Sm_2(SO_4)_3.8H_2O$ + (0.50mmol) H_6TTHA + (556mmol) H_2O	180	72	colorless block
XIa	(0.30 mmol) $Pr_2(SO_4)_3.8H_2O$ + (0.30mmol) H_6TTHA + (556mmol) H_2O	180	48	light green square block
XIb	(0.30 mmol) $Nd_2(SO_4)_3.8H_2O$ + (0.30mmol) H_6TTHA + (556mmol) H_2O	180	48	light purple square block
XII	(0.30 mmol) $Sm_2(SO_4)_3.8H_2O$ + (0.30mmol) H_6TTHA + (556mmol) H_2O	180	48	Colorless block

6.1.2 Single Crystal Structure Determination

Intensity data sets of **IXa**, **X**, **XIa**, and **XII** were collected in series of ω–scans using a Stöe IPDS2 image plate diffractometer and Mo $K\alpha$ radiation at 150(2) K. The collected data were analytically corrected for absorption using the Tompa method [14]. The single crystal data of **IXb** and **XIb** which are isostructure to **IXa** and **XIa**, respectively were on the other hand collected on a Bruker SMART Apex CCD diffractometer at 293(2) K. All structures were then solved by direct methods within SHELXS–97 [15] and full–matrix least squares refinement carried out within SHELXL–97 [16] *via* the WinGX program interface [17]. All non–hydrogen positions were located in the direct and difference Fourier maps and refined as anisotropic thermal parameters. The hydrogen atoms of the organic moieties were apparent from difference Fourier maps and refined using the riding mode. Selected details on the structure solution and refinements for every compound are listed in Table 6.2. The refined atomic coordinates and equivalent isotropic displacement parameters for the low temperature data of **IXa**, **X**, **XIa** and **XII** are provided in Table 6.3–6.6. Table 6.7–6.10 list selected bond distances about the metal centers for the reported compounds. Based on the refined bond distances with a single point energy model, the bond valence sums have been calculated [18], indicating the trivalence for every metal centers as listed;

IXa; BVS for Pr(1) = 3.37 and Pr(2) = 3.77,

X; BVS for Sm(1) = 3.13, Sm(2) = 3.31, Sm(3) = 3.45 and Sm(4) = 3.68,

XIa BVS for Pr(1) = 3.39 and Pr(2) = 3.79,

XII; BVS for Sm(1) = 3.31.

Table 6.2 Crystal data and structure refinement parameters for **IXa**, **IXb, X, XIa, XIb** and **XII**

Identification code	**IXa**	**IXb**	**X**	**XIa**	**XIb**	**XII**
Empirical formula	$C_{34}H_{29}N_{13}O_{35}Pr_4$	$C_{34}H_{29}N_{13}O_{35}Nd_4$	$C_{64}H_{53}N_{25}O_{63}Sm_8$	$C_{30}H_{30}N_{12}O_{36}Pr_4S$	$C_{30}H_{24}N_{12}O_{36}Nd_4S$	$C_{15}H_{12}N_6O_{25}Sm_2$
Formula weight	1743.34	1756.66	3382.11	1730.36	1737.63	977.01
Crystal system	Triclinic	Triclinic	Triclinic	Triclinic	Triclinic	monoclinic
Space group	$P\bar{1}$	$P\bar{1}$	$P\bar{1}$	$P\bar{1}$	$P\bar{1}$	$C2/c$
a/ Å	9.9245(12)	9.9171(15)	11.4156(9)	9.7887(9)	9.7547(4)	12.6974(13)
b/ Å	11.0004(14)	11.0222(17)	13.7226(10)	10.0556(10)	10.0569(5)	16.7309(12)
c/ Å	13.8484(16)	13.819(2)	17.4115(14)	12.4566(11)	12.4275(6)	14.8076(15)
α/°	77.599(10)	77.370(4)	76.985(6)	92.514(8)	92.5470(10)	90.00
β/°	79.108(9)	78.795(4)	82.578(6)	91.623(7)	91.7890(10)	91.452(8)
γ/°	66.395(9)	66.102(4)	88.768(6)	91.495(8)	91.3620(10)	90.00
Volume/ Å^3	1344.1(3)	1338.1(4)	2635.1(4)	1224.0(2)	1216.98(10)	3144.7(5)
Z	1	1	1	1	1	4
T/K	150(2)	293(2)	150(2)	150(2)	293(2)	150(2)
ρ_{calc} (g cm^{-3})	2.154	2.180	2.131	2.348	2.371	2.064
μ (mm^{-1})	3.676	3.931	4.497	4.077	4.363	3.805
θ range(°)	2.85–34.75	2.75–34.82	2.55–27.07	2.55–34.70	2.03–30.65	2.45–34.80
λ (Mo Kα) (Å)	0.71073	0.71073	0.71073	0.71073	0.71073	0.71073
R_{int}	0.0644	0.0404	0.0800	0.0432	0.0144	0.0534
reflection collected	11388	5506	11493	5901	7357	6737
unique reflections	8265	4378	8030	4910	6537	4680
no. of parameters	423	410	721	401	395	228
R, Rw (I>2σ(I))	0.0479, 0.1124	0.0700, 0.1654	0.0603, 0.1529	0.0371, 0.0963	0.0336, 0.0974	0.0542, 0.1250
R, Rw (all data)	0.0750, 0.1237	0.0898, 0.1818	0.0915, 0.1692	0.0478, 0.1008	0.0398, 0.1070	0.0901, 0.1461
Goodness of fit	1.054	1.117	1.031	1.065	1.144	1.081

Table 6.3 Atomic coordinates (×10^4) and equivalent isotropic displacement parameters (Å^2 × 10^3) for **IXa**.

	x	*y*	*z*	*U(eq)*
Pr(1)	4734(1)	1794(1)	4112(1)	16(1)
Pr(2)	5925(1)	6212(1)	8828(1)	19(1)
O(1)	4970(4)	2503(3)	5705(3)	22(1)
O(2)	5549(4)	333(3)	5831(3)	21(1)
O(3)	5059(5)	5524(5)	10783(3)	41(1)
O(4)	6374(5)	6781(5)	10410(3)	35(1)
O(5)	6741(3)	2786(3)	3793(3)	21(1)
O(6)	4032(4)	7193(4)	7605(3)	28(1)
O(7)	8239(3)	6704(4)	8442(3)	23(1)
O(8)	3172(3)	2350(3)	2766(3)	22(1)
O(9)	7406(3)	4762(3)	7524(3)	22(1)
O(10)	3475(4)	4186(3)	3920(3)	27(1)
O(11)	7151(4)	84(3)	3742(3)	28(1)
O(12)	2494(3)	1830(3)	5190(3)	22(1)
O(13)	7919(6)	4113(5)	9544(5)	60(2)
O(15)	3438(9)	7766(8)	9613(6)	35(2)
O(17)	–1359(11)	10348(11)	8397(7)	47(2)
O(1W)	5000	5000	5000	60(2)
O(2W)	1417(6)	9028(7)	4731(6)	71(2)
N(1)	4306(4)	2503(4)	7719(3)	21(1)
N(2)	755(4)	6751(4)	7204(3)	21(1)
N(3)	59(4)	3148(4)	6487(4)	27(1)
N(4)	2138(4)	2767(4)	7177(3)	22(1)
N(5)	2541(4)	4641(4)	7496(3)	21(1)
N(6)	391(4)	5007(4)	6758(3)	21(1)
N(7)	1366(11)	10159(9)	9935(7)	36(2)
C(1)	5195(4)	1385(4)	6228(3)	18(1)
C(2)	5018(5)	1228(4)	7351(3)	21(1)
C(3)	4508(5)	3635(5)	8997(3)	25(1)
C(4)	5179(5)	3118(5)	8018(3)	21(1)
C(5)	3058(4)	7163(4)	7129(3)	20(1)
C(6)	1594(5)	7190(5)	7712(4)	21(1)
C(7)	–1936(4)	7305(4)	7568(3)	19(1)
C(8)	–687(5)	7625(4)	6899(4)	22(1)
C(9)	–2501(4)	4935(4)	6595(3)	19(1)
C(10)	–1197(5)	4034(5)	5969(4)	26(1)
C(11)	2106(5)	1125(5)	5932(4)	23(1)

Table 6.3 Atomic coordinates (×10^4) and equivalent isotropic displacement parameters (Å^2 × 10^3) for **IXa** (continued).

	x	*y*	*z*	*U(eq)*
C(12)	584(5)	1714(5)	6505(5)	29(1)
C(13)	887(5)	3667(5)	6813(4)	22(1)
C(14)	2944(4)	3334(4)	7452(3)	19(1)
C(15)	1240(4)	5421(4)	7151(3)	20(1)
C(16)	3779(15)	8806(13)	9426(12)	49(2)
C(17)	2794(13)	10159(13)	9790(11)	60(5)
C(18)	673(19)	10385(13)	9047(8)	45(3)
C(19)	–812(17)	10191(12)	9130(9)	46(3)
O(3WA)	10380(40)	4440(30)	9820(30)	188(14)
O(3WB)	10729(11)	3301(14)	9778(8)	54(3)
O(14)	4985(11)	8740(8)	8896(7)	42(2)
O(16)	4203(13)	8455(11)	9145(9)	49(2)

Table 6.4 Atomic coordinates (×10^4) and equivalent isotropic displacement parameters (Å^2 × 10^3) for **X**.

	x	*y*	*z*	*U(eq)*
Sm(1)	5100(1)	8862(1)	1048(1)	26(1)
Sm(2)	6412(1)	5950(1)	1739(1)	13(1)
Sm(3)	8414(1)	4268(1)	3242(1)	14(1)
Sm(4)	9621(1)	1367(1)	3846(1)	22(1)
O(1)	4237(7)	8491(5)	2453(4)	23(2)
O(2)	5419(6)	7310(5)	2209(4)	18(1)
O(3)	5200(9)	10420(6)	1578(5)	34(2)
O(4)	5326(11)	10764(7)	291(5)	49(3)
O(5)	7071(12)	9170(10)	1316(10)	77(4)
O(6)	3136(12)	9589(11)	1069(7)	67(3)
O(7)	6522(7)	7666(6)	571(5)	31(2)
O(8)	3704(6)	7560(5)	1070(4)	19(1)
O(9)	4586(6)	6079(6)	1225(4)	21(2)
O(10)	7332(6)	5955(5)	2908(4)	18(1)
O(11)	6929(6)	6208(6)	257(4)	21(1)
O(12)	8443(6)	6353(6)	1359(4)	25(2)
O(13)	5249(6)	4921(5)	2832(4)	17(1)
O(14)	7502(6)	4285(5)	2073(4)	18(1)

Table 6.4 Atomic coordinates (×10^4) and equivalent isotropic displacement parameters (Å^2 × 10^3) for **X** (continued).

	x	***y***	***z***	***U(eq)***
O(15)	6163(6)	4346(5)	1276(4)	17(1)
O(16)	8632(7)	5831(5)	3743(4)	21(1)
O(17)	9572(6)	5316(5)	2122(4)	20(1)
O(18)	7976(6)	3909(5)	4778(4)	22(2)
O(19)	10259(6)	4159(6)	3692(5)	27(2)
O(20)	8255(6)	2598(5)	4249(4)	21(2)
O(21)	6370(6)	3914(6)	3643(4)	28(2)
O(22)	9431(6)	2925(5)	2705(4)	18(1)
O(23)	11109(6)	2669(6)	3855(4)	21(1)
O(24)	10578(7)	1693(5)	2486(4)	24(2)
O(25)	11712(15)	839(7)	3900(6)	71(4)
O(26)	9917(8)	1044(6)	5147(4)	32(2)
O(27)	9792(8)	–308(6)	3617(5)	30(2)
O(28)	7905(9)	1046(7)	3231(7)	47(2)
O(29A)	7764(15)	410(12)	4428(10)	28(3)
O(29B)	7880(20)	372(17)	4822(14)	51(5)
O(30)	5823(16)	–1643(13)	4507(10)	35(4)
O(1W)	5000	5000	0	54(4)
O(2W)	0	5000	5000	45(4)
O(3W)	8777(10)	4739(9)	242(6)	53(3)
C(1)	4617(9)	7631(7)	2655(5)	17(2)
C(2)	4117(9)	6924(8)	3437(5)	18(2)
C(3)	2114(8)	6999(7)	5168(5)	16(2)
C(4)	2790(9)	7681(8)	4411(6)	19(2)
C(5)	–336(9)	8969(7)	4202(6)	20(2)
C(6)	–1062(9)	8073(8)	4193(6)	22(2)
C(7)	–1988(8)	6362(8)	3274(6)	18(2)
C(8)	–1956(9)	7482(7)	3122(6)	19(2)
C(9)	3697(9)	6623(7)	1213(5)	16(2)
C(10)	2537(8)	6053(7)	1352(6)	17(2)
C(11)	–577(9)	6050(8)	1578(6)	22(2)
C(12)	492(9)	6642(9)	1105(6)	23(2)
C(13)	2042(8)	7197(7)	3322(5)	15(2)
C(14)	154(8)	7541(7)	3139(5)	13(2)
C(15)	1333(8)	6917(7)	2238(5)	16(2)
C(16)	5413(9)	4193(8)	3403(5)	18(2)
C(17)	4328(8)	3605(8)	3873(6)	21(2)

Table 6.4 Atomic coordinates ($\times 10^4$) and equivalent isotropic displacement parameters ($\text{Å}^2 \times 10^3$) for **X** (continued).

	x	*y*	*z*	*U(eq)*
C(18)	1150(8)	3592(8)	3711(5)	18(2)
C(19)	2313(8)	4164(8)	3569(6)	18(2)
C(20)	5464(11)	1007(8)	934(6)	25(2)
C(21)	6000(9)	2024(7)	864(6)	18(2)
C(22)	6826(8)	3859(7)	1731(5)	17(2)
C(23)	6827(9)	2708(7)	1907(6)	19(2)
C(24)	2973(9)	2868(9)	–120(6)	23(2)
C(25)	2155(9)	2331(8)	620(6)	22(2)
C(26)	247(9)	2588(7)	2269(5)	17(2)
C(27)	825(8)	3233(8)	1488(5)	19(2)
C(28)	3538(8)	3250(7)	2751(6)	16(2)
C(29)	4729(8)	2586(7)	1896(6)	15(2)
C(30)	2862(8)	2914(7)	1675(6)	18(2)
C(31)	7340(20)	538(18)	3794(10)	36(5)
C(32)	6240(20)	160(20)	3602(14)	41(6)
C(33)	5120(20)	940(20)	4453(16)	37(5)
N(3)	1485(7)	6603(7)	1552(5)	22(2)
C(34)	5460(20)	–860(20)	4732(16)	39(6)
N(1)	2951(7)	7229(6)	3737(5)	18(2)
N(2)	–955(7)	7846(6)	3405(5)	17(2)
N(4)	281(7)	7303(6)	2435(5)	19(2)
N(5)	999(7)	7535(6)	3602(5)	18(2)
N(6)	2250(7)	6826(6)	2665(5)	15(2)
N(7)	3347(7)	3596(7)	3422(5)	18(2)
N(8)	5842(7)	2318(6)	1619(5)	15(2)
N(9)	1981(8)	2883(7)	1231(5)	20(2)
N(10)	4601(7)	2869(6)	2581(5)	17(2)
N(11)	3899(7)	2546(6)	1424(5)	16(2)
N(12)	2637(7)	3333(6)	2311(5)	19(2)
N(13)	5473(19)	29(16)	4290(12)	38(5)

Table 6.5 Atomic coordinates ($\times 10^4$) and equivalent isotropic displacement parameters ($Å^2 \times 10^3$) for **XIa**.

	x	*y*	*z*	*U(eq)*
Pr(1)	548(1)	895(1)	8552(1)	12(1)
Pr(2)	973(1)	3391(1)	5943(1)	25(1)
O(1)	3456(4)	2816(5)	6228(3)	28(1)
O(2)	2128(4)	1731(4)	7289(3)	20(1)
O(3)	–764(4)	2252(5)	6990(4)	31(1)
O(4)	–1921(4)	1354(4)	8272(4)	25(1)
O(5)	784(4)	901(4)	10629(3)	20(1)
O(6)	2613(4)	1630(4)	9834(3)	23(1)
O(7)	2165(6)	3281(6)	4169(3)	42(1)
O(8)	–492(5)	5368(6)	5978(4)	38(1)
O(9)	2154(6)	–842(5)	8744(4)	38(1)
O(10)	2261(10)	–2585(6)	7633(5)	78(3)
O(11)	433(4)	3254(4)	9044(3)	20(1)
O(12)	1355(4)	4453(4)	7756(3)	25(1)
O(13)	102(4)	–591(4)	6920(3)	23(1)
O(14)	756(9)	636(8)	5345(6)	24(2)
O(15)	1875(13)	–1374(14)	5825(11)	63(4)
O(16)	–393(12)	–1494(10)	5147(7)	42(3)
O(17)	1065(9)	–2603(8)	5228(6)	25(2)
O(18)	2465(6)	5450(6)	5975(5)	47(1)
O(1WA)	–5010(20)	6780(20)	5702(16)	88(4)
O(1WB)	–5040(20)	6170(20)	5428(16)	88(4)
O(2W)	5020(90)	–530(50)	9660(40)	750(60)
C(1)	3313(5)	2111(5)	7020(4)	16(1)
C(2)	4549(5)	1667(5)	7657(4)	17(1)
C(3)	–1881(5)	1978(5)	7411(5)	21(1)
C(4)	–3211(5)	2320(5)	6843(4)	18(1)
C(5)	2013(5)	1377(5)	10668(4)	15(1)
C(6)	2700(6)	1709(5)	11754(4)	17(1)
C(7)	1344(6)	3886(6)	3603(4)	20(1)
C(8)	1312(5)	3639(5)	2400(4)	18(1)
C(9)	2405(7)	–2026(6)	8552(5)	29(1)
C(10)	2883(7)	–2802(6)	9498(5)	27(1)
C(11)	1248(5)	4132(5)	8713(4)	15(1)
C(12)	2161(6)	4806(5)	9591(4)	17(1)
C(13)	–4426(5)	3864(5)	7971(4)	15(1)
C(14)	–3622(5)	5980(5)	8129(4)	16(1)

Table 6.5 Atomic coordinates ($\times 10^4$) and equivalent isotropic displacement parameters (Å^2 × 10^3) for **XIa** (continued).

	x	*y*	*z*	*U(eq)*
C(15)	–5715(5)	5445(5)	8768(4)	15(1)
N(1)	–4301(4)	2601(4)	7579(4)	17(1)
N(2)	–2587(5)	6855(4)	8004(3)	16(1)
N(3)	3138(5)	5806(4)	9260(4)	17(1)
N(4)	–5575(5)	4143(4)	8506(4)	16(1)
N(5)	–3413(5)	4724(4)	7782(3)	17(1)
N(6)	–4776(5)	6403(4)	8581(4)	18(1)
S(1)	566(3)	–666(3)	5815(2)	26(1)

Table 6.6 Atomic coordinates ($\times 10^4$) and equivalent isotropic displacement parameters (Å^2 × 10^3) for **XII**.

	x	*y*	*z*	*U(eq)*
Sm(1)	3769(1)	1984(1)	554(1)	14(1)
O(1)	3269(4)	715(2)	1362(3)	21(1)
O(2)	3786(4)	1729(3)	2194(3)	22(1)
O(3)	4775(3)	2672(3)	–645(3)	21(1)
O(4)	1929(3)	2169(2)	797(3)	16(1)
O(5)	2913(3)	1144(2)	–562(3)	18(1)
O(6)	3557(3)	3301(2)	1145(3)	20(1)
O(7)	4946(4)	927(3)	–3(3)	27(1)
O(8)	5500(3)	2277(3)	1206(3)	24(1)
O(1W)	5000	3773(4)	2500	33(2)
O(2W)	8868(5)	853(4)	548(5)	49(2)
O(3W)	6977 (4)	703(4)	–486(4)	40(1)
O(4W)	5458(5)	4919(4)	1214(5)	51(2)
O(5AW)	7465(13)	2081(12)	–1070(12)	60(4)
O(5BW)	7522(17)	2425(10)	–690(15)	69(5)
N(1)	3269(4)	–310(3)	2873(3)	19(1)
N(2)	5000	–2707(4)	2500	21(1)
N(3)	5000	–290(4)	2500	20(1)
N(4)	4087(4)	–1530(3)	2679(3)	20(1)
C(1)	3474(4)	1006(3)	2129(4)	19(1)
C(2)	3332(5)	545(3)	2990(3)	19(1)
C(3)	6018(4)	–2862(3)	1126(3)	15(1)
C(4)	5886(4)	–3112(3)	2103(3)	18(1)
C(5)	2217(4)	–1231(3)	3840(3)	17(1)
C(6)	2282(4)	–729(4)	2977(4)	20(1)
C(7)	4148(4)	–732(3)	2680(3)	18(1)
C(8)	5000	–1889(5)	2500	19(1)

Table 6.7 Selected bond distances in the compound **IXa**.

Bond distance (Å)[a]			
Pr(1)–O(10)	2.398(3)	Pr(2)–O(16)	2.451(11)
Pr(1)–O(12)	2.423(3)	Pr(2)–O(7)	2.502(3)
Pr(1)–O(11)	2.427(3)	Pr(2)–O(9)	2.514(3)
Pr(1)–O(2)^{i}	2.449(3)	Pr(2)–O(13)	2.516(5)
Pr(1)–O(8)	2.468(3)	Pr(2)–O(6)	2.522(4)
Pr(1)–O(5)	2.561(3)	Pr(2)–O(4)	2.563(4)
Pr(1)–O(1)	2.571(3)	Pr(2)–O(15)	2.569(7)
Pr(1)–O(2)	2.636(3)	Pr(2)–O(14)	2.572(8)
Pr(1)–O(6)^{ii}	2.692(4)	Pr(2)–O(8)^{ii}	2.659(4)
Pr(2)–O(3)^{iii}	2.397(4)	Pr(2)–O(3)	2.720(4)

[a] Symmetry codes: (i) [–*x* + 1, –*y*, –*z* + 1] (ii) [–*x* + 1, –*y* + 1, –*z* + 1] (iii) [–*x* + 1, –*y* + 1, –*z* + 2].

Table 6.8 Selected bond distances in the compound **X**.

Bond distance (Å)[a]			
Sm(1)–O(4)^{i}	2.383(9)	Sm(3)–O(19)	2.331(7)
Sm(1)–O(8)	2.410(7)	Sm(3)–O(21)	2.376(7)
Sm(1)–O(5)	2.420(14)	Sm(3)–O(14)	2.397(7)
Sm(1)–O(6)	2.434(14)	Sm(3)–O(17)	2.402(7)
Sm(1)–O(1)	2.460(7)	Sm(3)–O(22)	2.455(6)
Sm(1)–O(7)	2.484(8)	Sm(3)–O(16)	2.519(7)
Sm(1)–O(3)	2.523(8)	Sm(3)–O(20)	2.547(7)
Sm(1)–O(2)	2.641(7)	Sm(3)–O(10)	2.584(7)
Sm(1)–O(4)	2.646(9)	Sm(3)–O(18)	2.591(7)
Sm(2)–O(9)	2.361(7)	Sm(4)–O(26)	2.275(7)
Sm(2)–O(13)	2.366(7)	Sm(4)–O(27)	2.419(8)
Sm(2)–O(12)	2.369(7)	Sm(4)–O(24)	2.425(7)
Sm(2)–O(2)	2.408(7)	Sm(4)–O(20)	2.432(7)
Sm(2)–O(10)	2.409(7)	Sm(4)–O(28)	2.443(10)
Sm(2)–O(11)	2.517(7)	Sm(4)–O(25)	2.486(16)
Sm(2)–O(15)	2.542(7)	Sm(4)–O(29A)	2.491(17)
Sm(2)–O(14)	2.564(7)	Sm(4)–O(23)	2.496(7)
Sm(2)–O(7)	2.736(9)	Sm(4)–O(22)	2.598(7)
		Sm(4)–O(29B)	2.63(2)

[a] Symmetry code: (i) [–*x* + 1, –*y* + 2, –*z*].

Table 6.9 Selected bond distances in the compound **XIa**.

Bond distance (Å) [a]			
Pr(1)–O(9)	2.395(5)	Pr(2)–O(3)	2.461(5)
Pr(1)–O(2)	2.400(4)	Pr(2)–O(12)	2.470(4)
Pr(1)–O(11)	2.430(4)	Pr(2)–O(8)	2.480(5)
Pr(1)–O(5)$^{\mathrm{i}}$	2.473(4)	Pr(2)–O(18)	2.500(6)
Pr(1)–O(4)	2.491(4)	Pr(2)–O(17)$^{\mathrm{ii}}$	2.527(8)
Pr(1)–O(13)	2.491(4)	Pr(2)–O(7)	2.527(5)
Pr(1)–O(5)	2.591(4)	Pr(2)–O(1)	2.532(4)
Pr(1)–O(6)	2.610(4)	Pr(2)–O(2)	2.667(4)
Pr(1)–O(3)	2.736(5)	Pr(2)–O(8)$^{\mathrm{iii}}$	2.781(5)
Pr(2)–O(16)$^{\mathrm{ii}}$	2.340(9)	Pr(2)–O(14)	2.837(8)

[a] Symmetry codes: (i) [$-x, -y, -z + 2$] (ii) [$-x, -y, -z + 1$] (iii) [$-x, -y + 1, -z + 1$].

Table 6.10 Selected bond distances in the compound **XII**.

Bond distance (Å) [a]			
Sm(1)–O(6)	2.390(4)	Sm(1)–O(7)	2.470(4)
Sm(1)–O(4)	2.394(4)	Sm(1)–O(3)	2.495(4)
Sm(1)–O(5)	2.408(4)	Sm(1)–O(1)	2.526(4)
Sm(1)–O(8)	2.428(4)	Sm(1)–O(4)$^{\mathrm{i}}$	2.589(4)
Sm(1)–O(2)	2.466(4)		

[a] Symmetry codes: (i) [$-x + 0.5, -y + 0.5, -z$].

6.2 Results and discussion

By carefully adjusting the hydrothermal reaction time and the Ln:H_6TTHA mole ratios, *i.e.* 72 h and Ln:H_6TTHA=2:1.6 for **IXa**, **IXb** and **X**, and 48 h and Ln:H_6TTHA=2:1 for **XIa**, **XIb** and **XII**, six new compounds which can be categorized into four distinct frameworks can be synthesized. The prolongation of the hydrothermal reaction time to 72 h (in comparison to 48 h) apparently led to the decomposition of the H_6TTHA molecules to a smaller dicarboxylate ligand (Figure 6.2); 2,5–dioxo–piperazine–1,4–diacetic acid ($C_8H_{10}N_2O_6$ or *L2* hereafter) [19]. The *in situ* synthesized *L2* acts as an auxiliary dicarboxylate ligand in the frameworks **IXa**, **IXb** and **X**. One intriguing feature from the crystallographic viewpoint is the fact that there present a rare type of disorder, *i.e.* a special case of the substitutional disordered [20], in the three framework structures. It is also apparent that the use of Pr^{III} and Nd^{III} leads to isostructure frameworks whereas Sm^{III} gives different results.

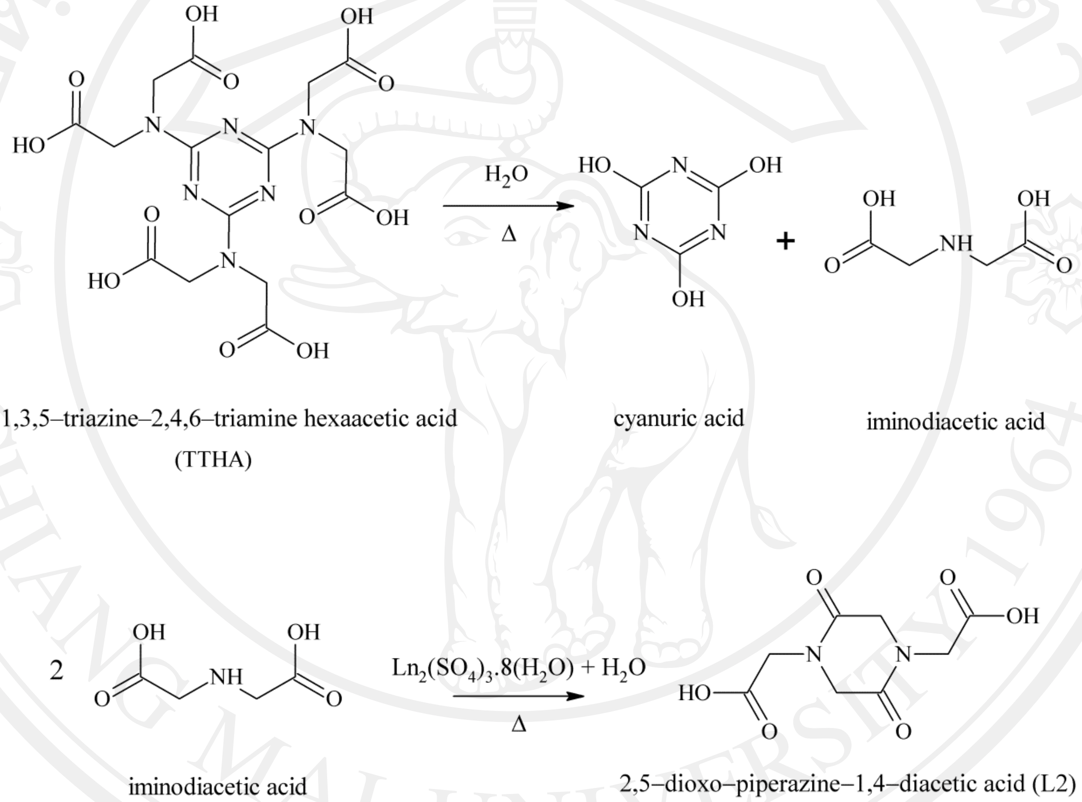

Figure 6.2 *In situ* synthesis of 2,5–dioxo–piperazine–1,4–diacetic acid (*L2*) from the decomposition reaction of the H_6TTHA ligand under the employed hydrothermal condition [19].

6.2.1 Crystal structures of $[Ln_4(C_{15}H_{12}O_{12}N_6)_2(C_8H_{10}N_2O_6)_{0.5}(H_2O)_3]\cdot5H_2O$, Ln = Pr^{III} (IXa) and Nd^{III} (IXb)

The compounds $[Ln_4(C_{15}H_{12}O_{12}N_6)_2(C_8H_{10}N_2O_6)_{0.5}(H_2O)_3]\cdot5H_2O$ where Ln = Pr^{III} (**IXa**) and Nd^{III} (**IXb**) are isostructure, crystallizing in the same triclinic $P\bar{1}$ space group with similar unit cell parameters (Table 6.2). A slightly smaller unit cell and therefore cell volume of **IXb** compared to **IXa** despite the higher temperature data set for the **IXb** case is clearly imparted from the lanthanide contraction. Here, only a detailed description of $[Pr_4(C_{15}H_{12}O_{12}N_6)_2(C_8H_{10}N_2O_6)_{0.5}(H_2O)_3]\cdot5H_2O$ (**IXa**) will be presented as a representative for the two isostructural compounds.

The asymmetric unit of **IXa** as shown in Figure 6.3 comprises as many as forty−three non−hydrogen atoms, including two independent Pr^{III} ions, a completely deprotonated TTHA hexavalent anion, a portion of *L2* ligand and water of crystallization. The two asymmetric Pr^{III} ions are located on the same Wyckoff position 2*i* and differentiated by the coordination number and environment. Pr(1) adopts the nine−fold pseudo−monocapped square anti−prismatic geometry which is fulfilled by nine O atoms from four symmetrically equivalent TTHA ligands. Contrary to Pr(1), the coordination about Pr(2) is rather complicated. The presence of the substitutional disorder at atoms O(14) and O(15) of the coordinated *L2* and the ligated water O(16) atom results in two different coordination environments, *i.e.* the nine−fold pseudo−monocapped square anti−prism and the ten−fold bicapped square anti−prism (Figure 6.3). As a result of such disorder, the coordination sphere of Pr(2) can be regarded as consisting of either one O atom from the ligated water molecule or two O atoms of the chelating *L2*. This type of crystallographic disorder as found in the structures of **IXa** (and **IXb)** is rather scarce, and only limited number of examples are known [21, 22]. Due to the presence of the small ligands in the coordination neighborhood of Pr(2), there are only three TTHA ligands coordinated to Pr(2) using seven O atoms.

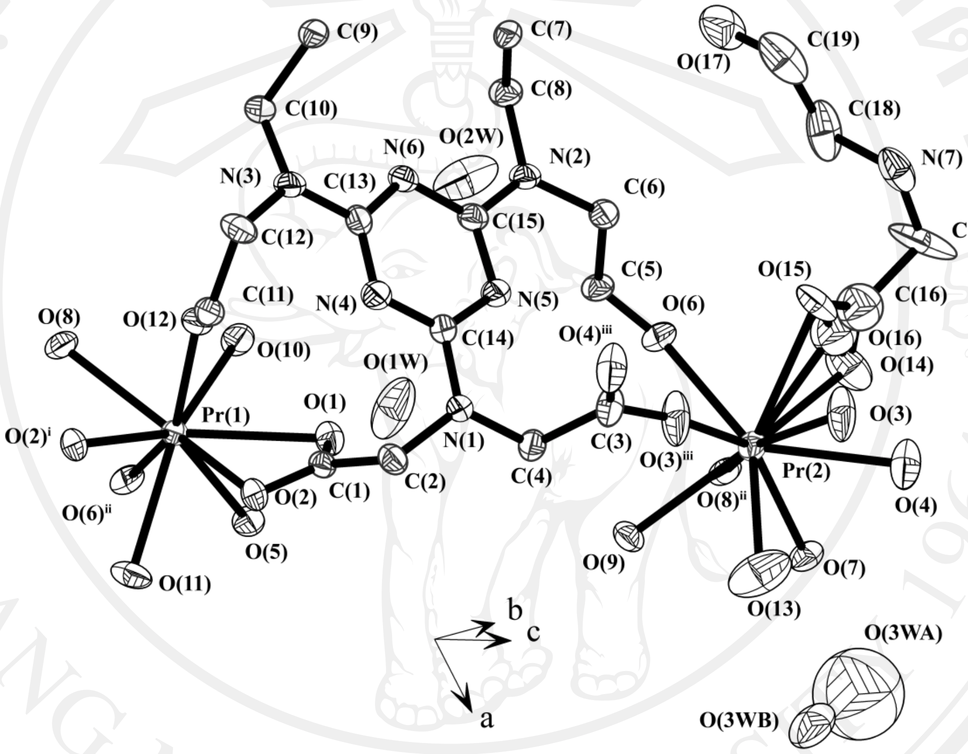

Figure 6.3 ORTEP view of coordination environments of $\mathrm{Pr^{III}}$ ions in **IXa** with displacement ellipsoids (60% probability) and atomic labeling for non–hydrogen atoms. Hydrogen atoms are omitted for clarity. Symmetry codes: (i) [–*x* + 1, –*y*, –*z* + 1] (ii) [–*x* + 1, –*y* + 1, –*z* + 1] (iii) [–*x* + 1, –*y* + 1, –*z* + 2].

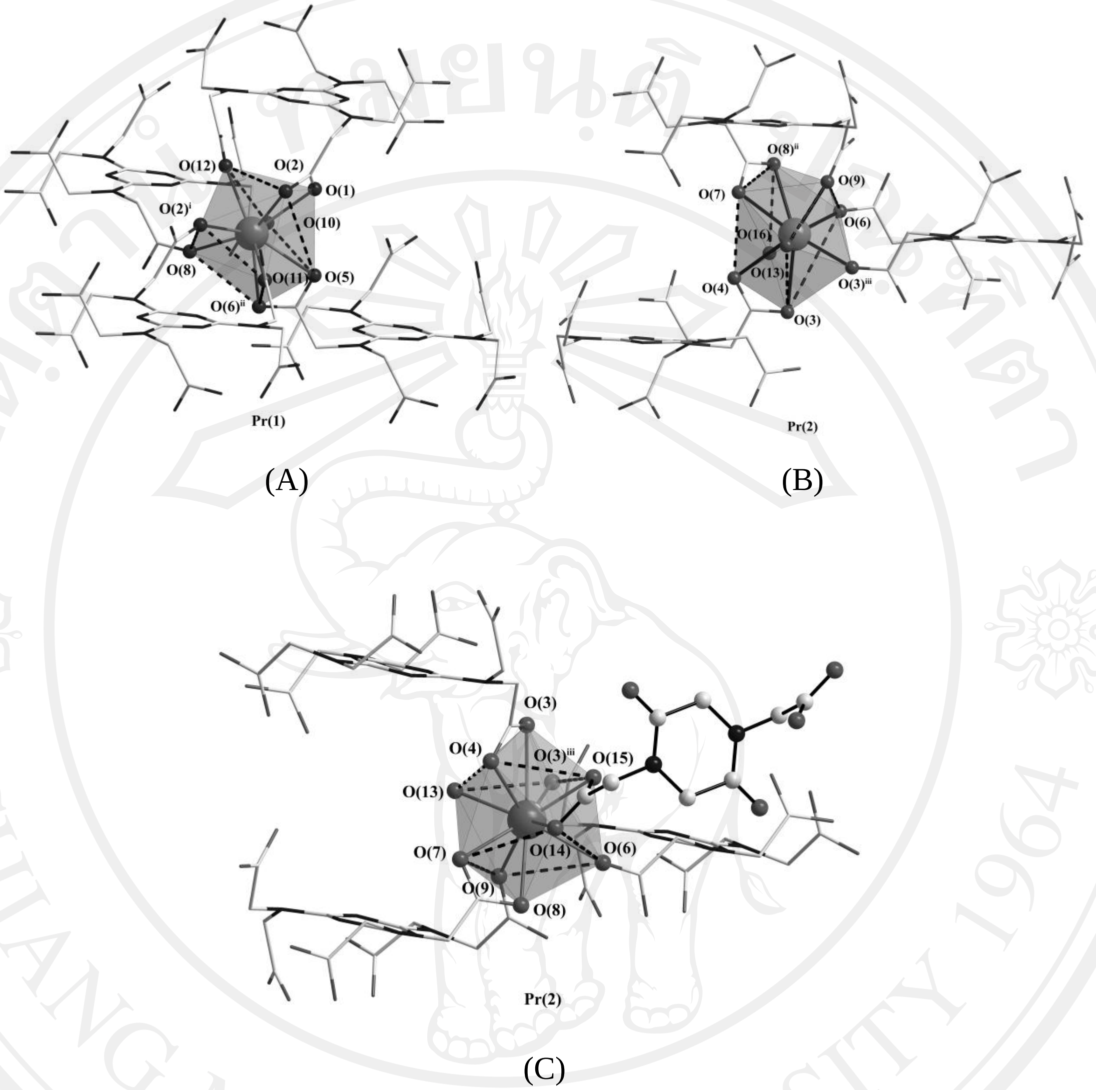

(A) (B)

(C)

Figure 6.4 View of (A) pseudo−monocapped square anti−prism of Pr(1) and (B) Pr(2), and (C) bicapped square anti−prism of Pr(2). Symmetry codes: (i) [−*x* + 1, −*y*, −*z* + 1] (ii) [−*x* + 1, −*y* + 1, −*z* + 1] (iii) [−*x* + 1, −*y* + 1, −*z* + 2].

Versatility in coordination modes, degree of protonation and relative conformation of the flexible carboxylato arms are important features of the flexible polycarboxylato ligands including TTHA. In the synthesis of **IXa**, the reaction was conducted in slightly acidic condition (pH = 4), the ligand is therefore completely deprotonated providing six free carboxylato arms to assemble four Pr(1) and three Pr(2) ions together as depicted in Figure 6.5. Concerning coordination modes of the TTHA's carboxylato O atoms in **IXa** as summarized in Table 6.11, there exist two different modes of coordination including $\mu_2-\eta^2:\eta^1$ and $\mu_2-\eta^1:\eta^1$ (*syn*−*syn*). It may be noted also that the conformation of the three pairs of the dicarboxylato arms anchored onto the common N atom are the same. For each pair, the dicarboxylato pendants are projected out of the molecular plane in a *trans* conformation with one arm pointing above and the other pointing below the plane (Figure 6.5).

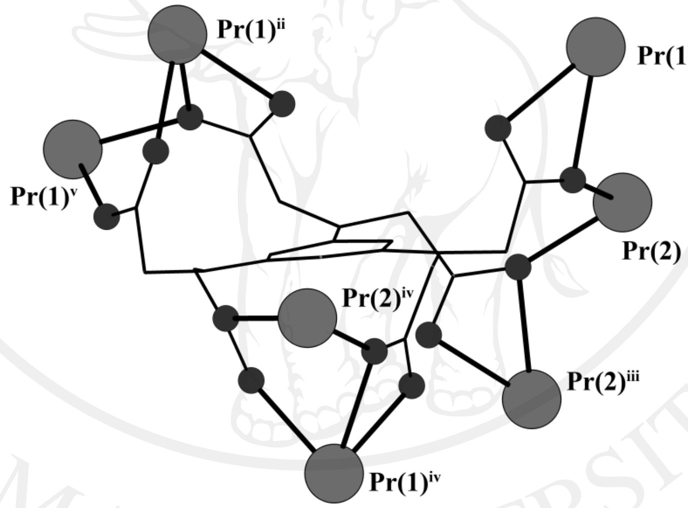

Figure 6.5 The assembly of four Pr(1) and three Pr(2) about the TTHA ligand in **IXa**. Symmetry codes: (ii) [–*x* + 1, –*y* + 1, –*z* + 1] (iii) [–*x* + 1, –*y* + 1, –*z* + 2] (iv) [*x* – 1, *y*, *z*] (v) [*x*, *y* – 1, *z*].

Table 6.11 Coordination modes of the carboxylates in TTHA and *L2* ligands.

	Coordination modes of carboxylato ligands				
	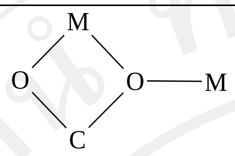 $\mu_2-\eta^2:\eta^1$	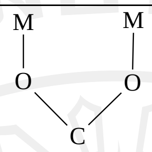 $\mu_2-\eta^1:\eta^1$ (*syn–syn*)	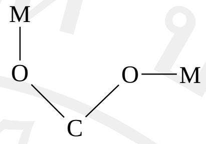 $\mu_2-\eta^1:\eta^1$ (*syn–anti*)	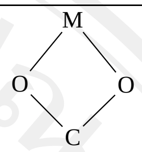 $\mu_1-\eta^1:\eta^1$	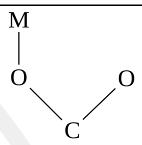 $\mu_1-\eta^1:\eta^0$
Compound IXa					
μ_7-η^{16}-TTHA	O(1)–C(1)–O(2) O(3)–C(3)–O(4) O(5)–C(5)–O(6) O(7)–C(7)–O(8)	O(9)–C(9)–O(10) O(11)–C(11)–O(12)			
L2				O(14)–C(16)–O(15)	
Compound X					
	O(1)–C(1)–O(2) O(18)–C(3)–O(20) O(10)–C(7)–O(16)	O(8)–C(9)–O(9) O(12)–C(11)–O(17)	O(26)–C(5)–O(27)		
μ_7-η^{16}-TTHA	O(3)–C(20)–O(4) O(14)–C(22)–O(15) O(7)–C(24)–O(11) O(22)–C(26)–O(24)	O(13)–C(16)–O(21) O(19)–C(18)–O(23)			
L2				O(28)–C(31)–O(29A)	
Compound XIa					
μ_8-η^{15}-TTHA	O(1)–C(1)–O(2) O(3)–C(3)–O(4) O(5)–C(5)–O(6) O(7)–C(7)–O(8)	O(11)–C(11)–O(12)			O(9)–C(9)–O(10)
Compound XII					
μ_6-η^{14}-TTHA	[O(3)–C(3)–O(4)] x 2	[O(5)–C(5)–O(6)] x 2		[O(1)–C(1)–O(2)] x 2	

The framework structure of **IXa** can be described as being constructed from three different dimers, *i.e.* {Pr(1)$_2$O$_{16}$}, {Pr(2)$_2$O$_{16}$} and {Pr(2)$_2$O$_{18}$}, as shown in Figure 6.6. As the {Pr(2)$_2$O$_{16}$} and {Pr(2)$_2$O$_{18}$} dimers are built up by fusing two corresponding {Pr(2)O$_9$} and {Pr(2)O$_{10}$} through only the shared edge generated from

O(3) by $\bar{1}$ symmetry, the $\{Pr(1)_2O_{16}\}$ dimer is established using both the common edge generated from O(2) and two symmetry equivalent $\mu_2-\eta^1:\eta^1$ (*syn–syn*) O(12)–C(11)–O(11) linkages. The dimers are then alternatively connected, using the shared edge (O(6)–O(8)) and the $\mu_2-\eta^1:\eta^1$ carboxylato bridge, O(10)–C(9)–O(9) bridge, to form an infinite 1–D chain extending in the [0 –½ ½] direction as depicted in Figure 6.7. These chains are spatially transfixed by the coordinated $\mu_7-\eta^{16}$ TTHA ligand. The auxiliary *L2* ligand in addition links the adjacent $\{Pr(2)_2O_{18}\}$ dimers using the chelating $\mu_1-\eta^1:\eta^1$ mode of coordination as depicted in Figure 6.8, which result in the formation of the other puckered 1–D chain in the [–½ ½ 0] direction. According to the FT–IR spectroscopic result, there present the characteristic absorptions of N–H at 3200 cm^{-1} as shown in Figure 6.9. This spectroscopic result then suggests the protonation at N atoms of the *L2* ligand which neutralizes charge of the framework.

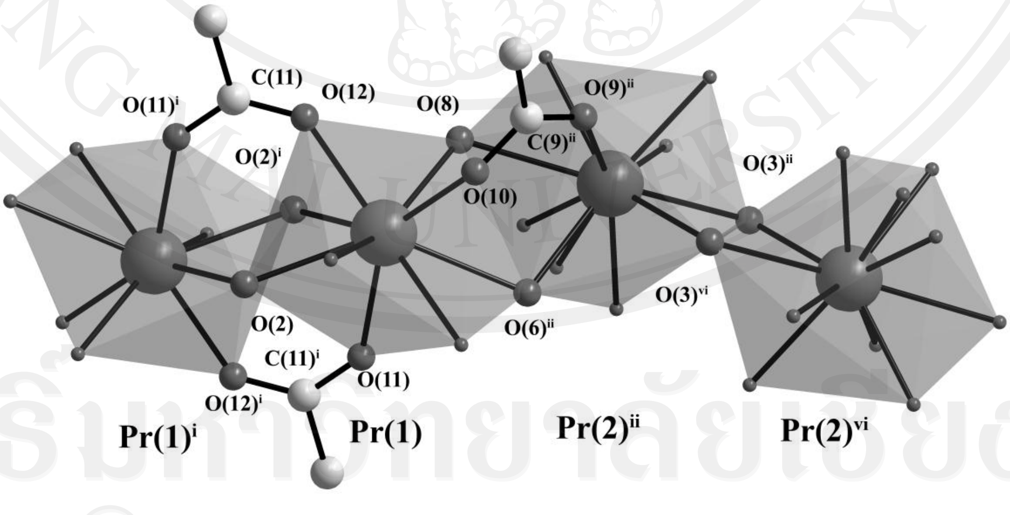

Figure 6.6 The structural building dimers in **IXa**; $\{Pr(1)_2O_{16}\}$, $\{Pr(2)_2O_{16}\}$ and $\{Pr(2)_2O_{18}\}$. Symmetry codes: (i) [$-x + 1, -y, -z + 1$] (ii) [$-x + 1, -y + 1, -z + 1$] (vi) [$x, y, z - 1$].

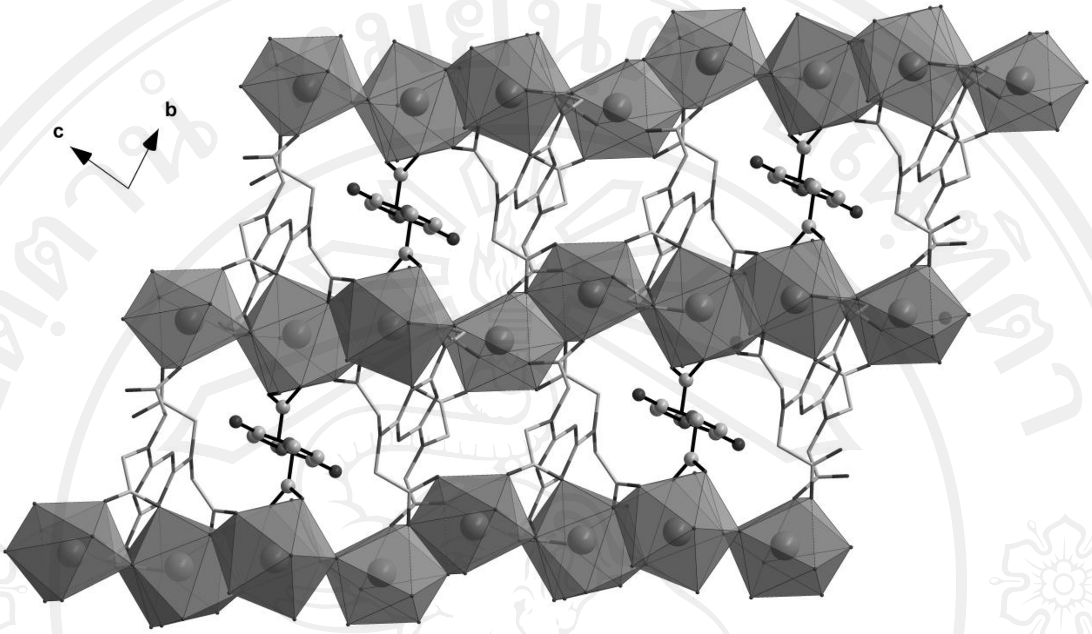

Figure 6.7 The infinite 1–D chains of regularly alternative $\{\mathrm{Pr(1)_2O_{16}}\}$ and $\{\mathrm{Pr(2)_2O_{16}}\}$ or $\{\mathrm{Pr(2)_2O_{18}}\}$ dimers extending along the [0 –½ ½] direction, which are linked by the μ_7–η^{16} TTHA ligands. Water of crystallization and hydrogen atoms are omitted for clarity.

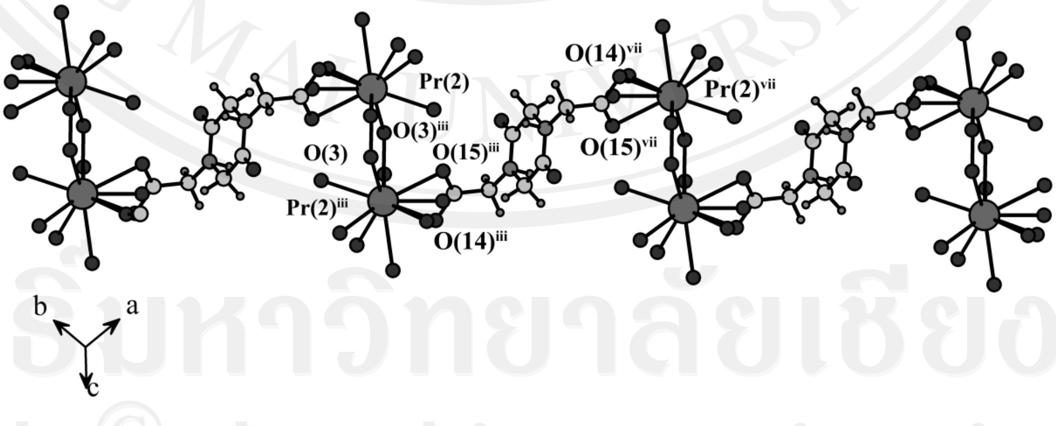

Figure 6.8 Infinite 1–D chains made up of the $\{\mathrm{Pr(2)_2O_{18}}\}$ dimers and the diprotonated *L2* ligands extending along the [–½ ½ 0] direction. Symmetry codes: (iii) [–*x* + 1, –*y* + 1, –*z* + 2] (vii) [x + 1, y – 1, z] .

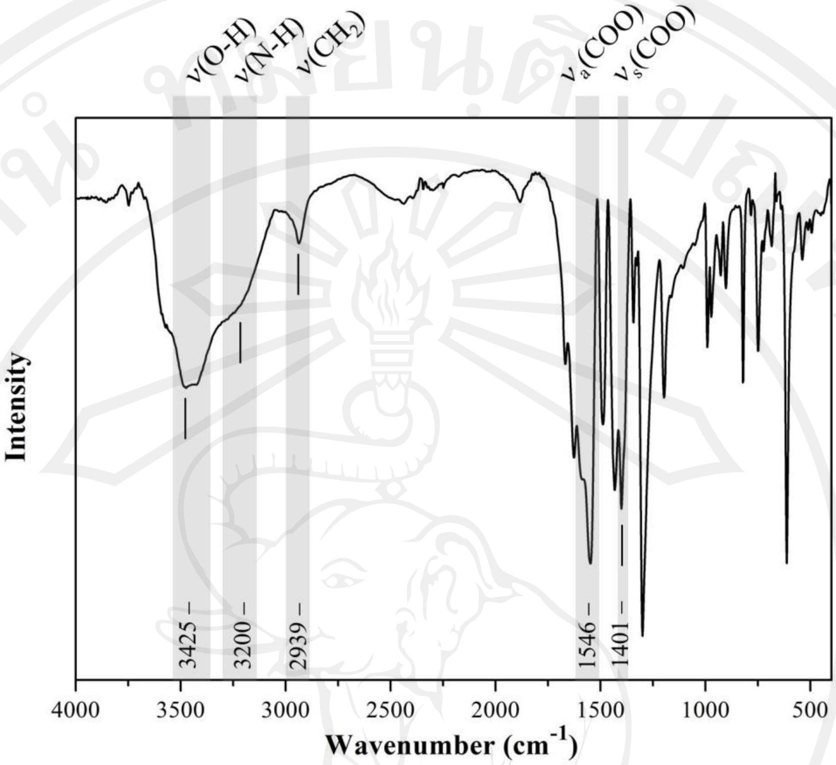

Figure 6.9 FT–IR spectrum of compound **IXa** with selected band indexing.

Revealing from the assembly of the extending 1–D chain as shown in Figure 6.10, the structure of **IXa** are dense 3–D framework with insignificant void of *ca.* 5.3% calculated using PLATON [23]. The free space is occupied by water of crystallization located in a close proximity to the dicarboxylato ligands of TTHA. The crystallizing water molecules apparently establish the hydrogen bonding interactions with the framework using the conventional O···O and N–H···O, and the very weak C–H···O interactions as listed in Table 6.12. Being a dense framework of highly populated dicarboxylato ligands as described, the established hydrogen bonding interactions should impart only minor influence in directing and stabilizing the framework architecture.

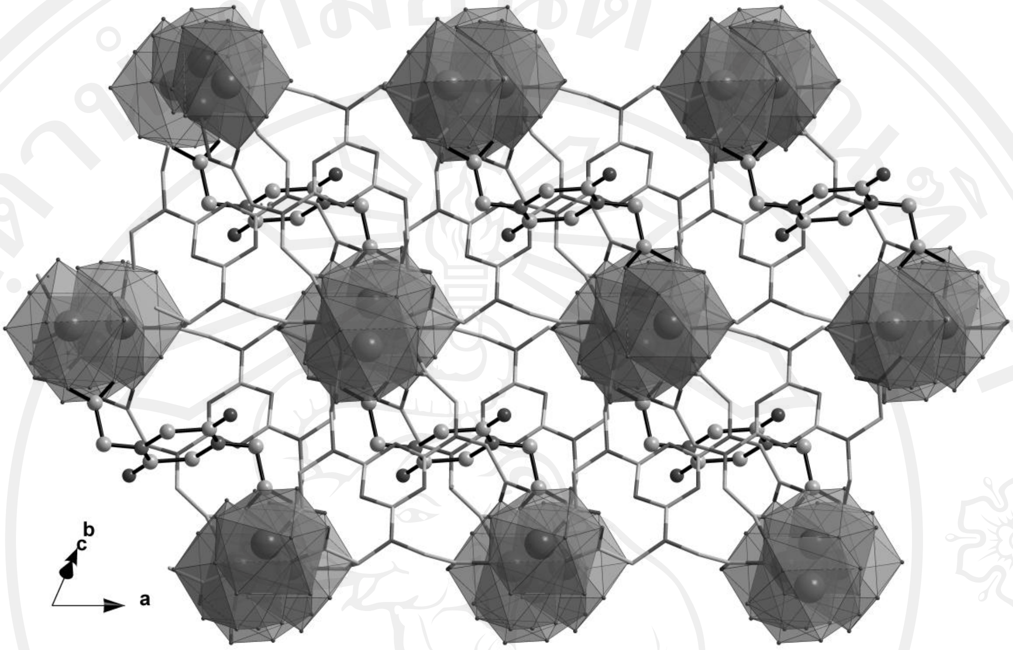

Figure 6.10 Dense 3–D framework structure of **IXa**. Water of crystallization and hydrogen atoms are omitted for clarity.

Table 6.12 List of hydrogen bonding interactions and geometries in **IXa**.

D – H ··· A [a]	D – H, (Å)	H ··· A, (Å)	D ··· A, (Å)	D – H ··· A, (°)
O(13) ··· O(3WA)	–	–	2.712 (45)	–
O(13) ··· O(3WB)	–	–	2.627(12)	–
N(7) – H(7) ··· O(3WB)^{i}	0.91	2.36	3.221(17)	159
C(2) – H(2A) ··· O(14)^{ii}	0.97	2.40	3.098(10)	129
C(12) – H(12A) ··· O(2W)^{iii}	0.97	2.32	3.275(9)	168

[a] symmetry codes: (i) [*x* – 1, *y* + 1, *z*] (ii) [*x*, *y* – 1, *z*] (iii) [–*x*, –*y* +1, –*z*] .

6.2.2 Crystal structure of $[Sm_8(C_{15}H_{12}O_{12}N_6)_4(C_8H_{10}N_2O_6)_{0.5}(H_2O)_8]\cdot 4H_2O$ (X)

The crystal structure of $[Sm_8(C_{15}H_{12}O_{12}N_6)_4(C_8H_{10}N_2O_6)_{0.5}(H_2O)_8]\cdot 4H_2O$ (**X**) can be solved and refined in the same triclinic $P\bar{1}$ space group as the structures **IXa** and **IXb** (Table 6.2) with however twice the volume of the unit cell. The asymmetric unit of **X** consists of as many as eighty non–hydrogen atoms from four crystallographically unique Sm^{III}, two non–equivalent TTHA ligands and half the molecule of *L2* ligand, as shown in Figure 6.11. Most of the asymmetric atoms are located on the Wyckoff position 2*i*, except O(W1) and O(W2) which are located on 1*e* and 1*g* positions, respectively.

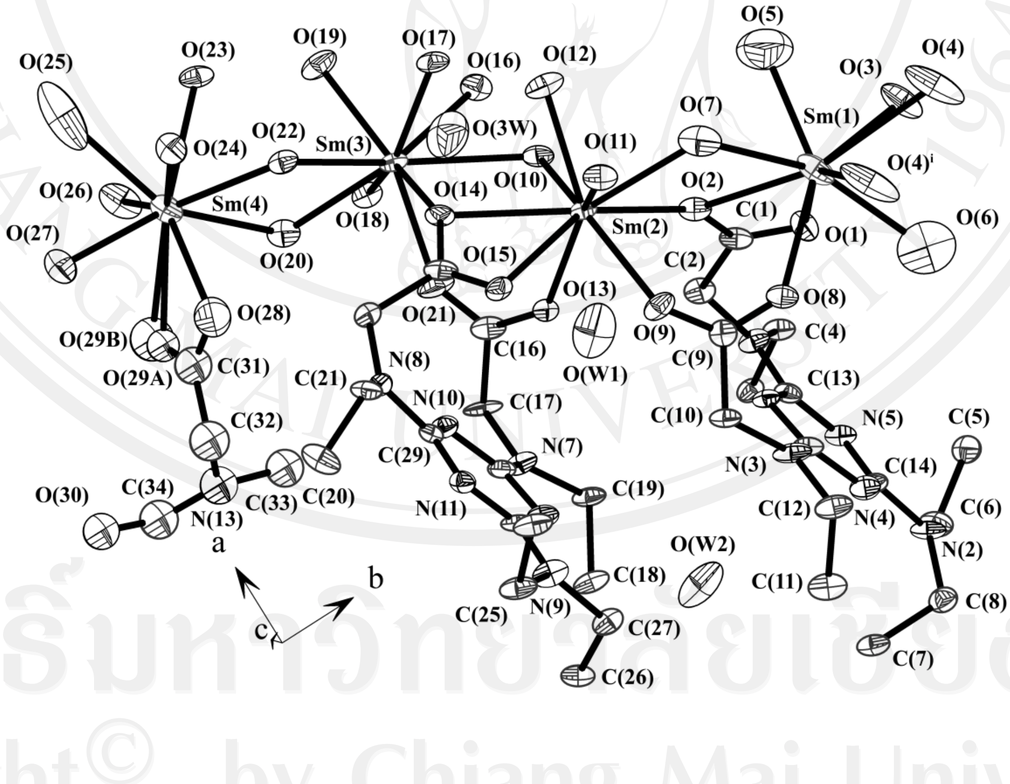

Figure 6.11 ORTEP view of the asymmetric unit of **X** with displacement ellipsoids (60% probability) and atomic labeling for non–hydrogen atoms. Hydrogen atoms are omitted for clarity. Symmetry code: (i) [$-x + 1, -y + 2, -z$].

Three Sm^{III} ions in **X**, *i.e*. Sm(1), Sm(2) and Sm(3) exhibit the same nine–fold pseudo–monocapped square anti–prismatic geometry as shown in Figure 6.12. The nine O atoms coordinated to Sm(1) are from two ligated water molecules (O(5) and O(6)) and three TTHA ligands of which four O atoms (O(3), O(4)×2 and O(7)) are from two equivalent TTHA and the other three (O(1), O(2) and O(8)) are of the other non–equivalent TTHA. The Sm(2) and Sm(3) ions share similar coordination neighborhood, which is crowded by nine O atoms from two pairs of two equivalent TTHA ligands. With reference to the surrounding of Sm(2), atoms O(2), O(9), O(10) and O(12) are from two equivalent TTHA, whereas atoms O(7), O(11), O(13), O(14) and O(15) are from the other two equivalent TTHA ligands. In a similar fashion, four O atoms, namely O(14), O(19), O(21) and O(22), are of the equivalent TTHAs while the other five O atoms, including O(10), O(16), O(17), O(18) and O(20), are of the other TTHA pair. Difference in bridging modes of the dicarboxylato arms about Sm(2) and Sm(3) distinguishes the two metal centers.

Contrary to Sm(1), Sm(2) and Sm(3), there present the substitutional disorder on atom O(28) and the commonly found site disorder on atoms O(29A) and O(29B) about the Sm(4) ion. Such disorder results in two alternative coordination environments about this metal center both of which are nine–fold pseudo–monocapped square anti–prismatic. This includes the O atom of one ligated water molecule (O(25)), six O atoms from three TTHA ligands, and two O atoms from either two independent ligated water molecules (O(29B) and O(28)) or the chelating auxiliary dicarboxylato ligand (O(29A) and O(28)). Among the six O atoms from three TTHA ligands, atoms O(20), O(26) and O(27) are from two equivalent TTHA whereas O(22), O(23) and O(24) are from the other independent TTHA.

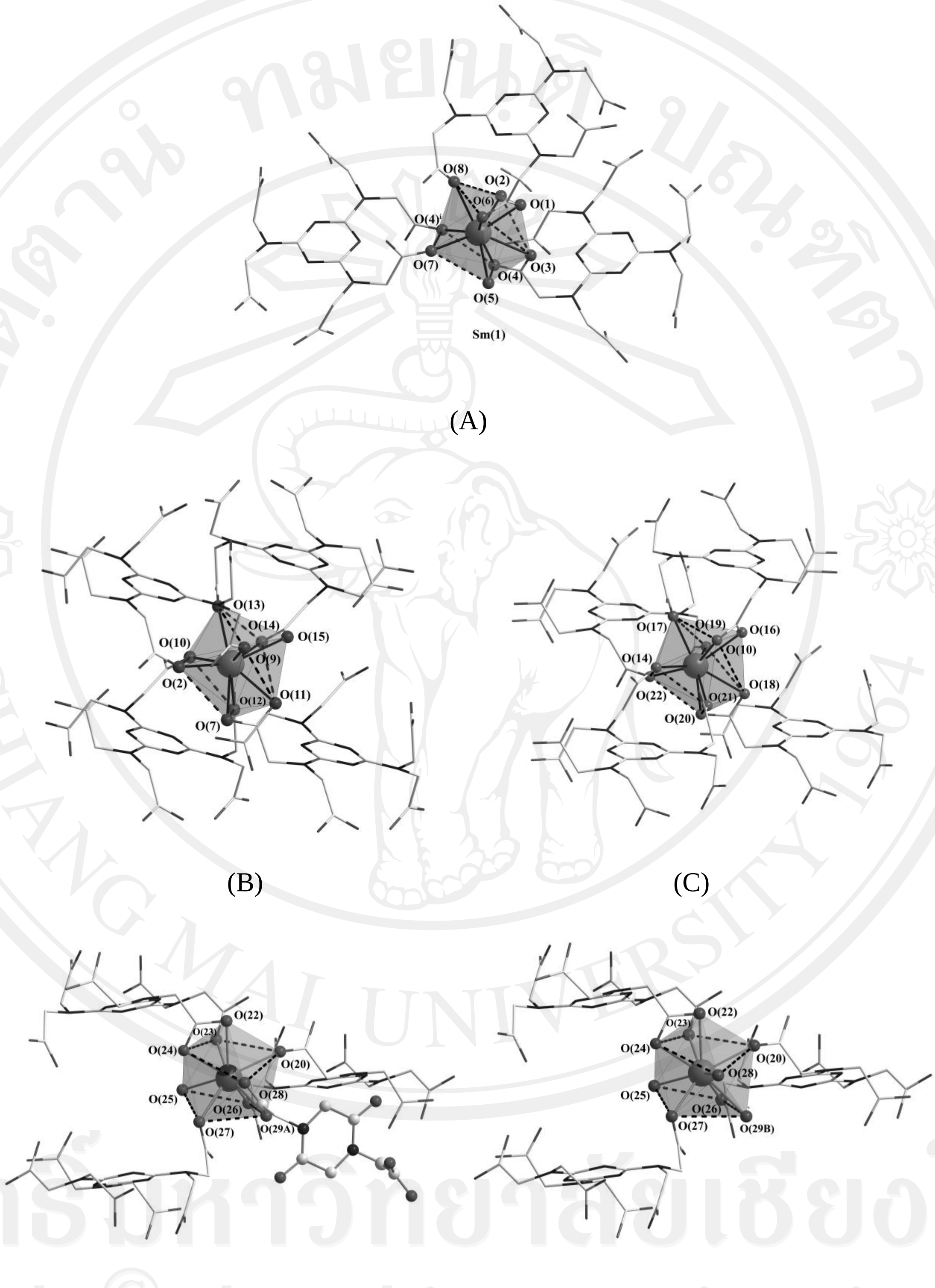

(A)

(B)

(C)

(D)

(E)

Figure 6.12 Pseudo–monocapped square anti–prismatic geometry of (A) Sm(1), (B) Sm(2), (C) Sm(3), (D) and (E) Sm(4). Symmetry code: (i) [–*x* + 1, –*y* + 2, –*z*].

If the ratio of Ln : TTHA : water/*L2* is to be considered, it may be intriguing to note the similarities in this ratio for the nine–fold coordinated metal centers of **IXa** which is isostructure to **IXb**, and those found in **X**. There present two different ratios for the Ln : TTHA : water/*L2* in these compounds, *i.e.* 1 : 4 : 0 for Pr(1), Sm(2) and Sm(3), and 1 : 3 : 2 for Pr(2) and Sm(1). The Ln : TTHA : water/*L2* for the nine–fold coordinated Sm(4) in structure **X** is on the other hand 1 : 3 : 3.

Due to the similar synthetic conditions (as **IXa** and **IXb**) adopted for the synthesis of **X**, the polycarboxylato ligands in this structure are also completely deprotonated providing completely free carboxylato O atoms to coordinate to the metals. In structure **X**, there are two distinct TTHA ligands differentiated by different modes of coordination as listed in Table 6.11. Although the $\mu_2-\eta^2:\eta^1$ and $\mu_2-\eta^1:\eta^1$ (*syn*−*syn*) are common between the two distinguish TTHA ligands, the additional $\mu_2-\eta^1:\eta^1$ (*syn*−*anti*) mode of coordination is found in the only one of them. The conformation of every dicarboxylato arms docked on the same N atom is also located in a *trans* fashion as diagrammatically illustrated in Figure 6.13, which is seemingly the preferred spatial orientations of the pendants. Accumulatively, each of the TTHA ligands in structure **X** connects seven Sm^{III} ions in the neighborhood, displaying one of the two different coordination modes, *i.e.* $\mu_7-\eta^{15}$ and $\mu_7-\eta^{16}$. While the $\mu_7-\eta^{15}$ TTHA connects Sm(1), Sm(2) × 2, Sm(3) × 2 and Sm(4) × 2 ions together, the $\mu_7-\eta^{16}$ TTHA links Sm(1) × 2, Sm(2) × 2, Sm(3) × 2 and one Sm(4).

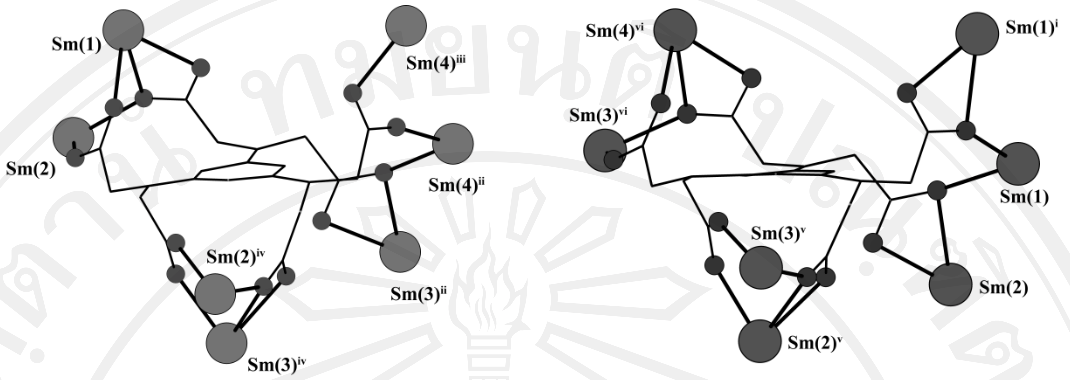

$\mu_7-\eta^{15}$ TTHA $\mu_7-\eta^{16}$ TTHA

Figure 6.13 View of coordination modes and relation conformation of carboxylate units in TTHA ligands found in structure **X**. Symmetry codes: (i) [$-x + 1, -y + 2, -z$] (ii) [$-x + 1, -y + 1, -z + 1$] (iii) [$-x + 1, y + 1, z$] (iv) [$x - 1, y, z$] (v) [$-x +1, -y + 1, -z$] (vi) [$-x + 2, -y + 1, -z$].

At first glance, the framework structure of **X** looks similar to that of **IXa** and **IXb**, there are however eminent differences between the two frameworks. The basic building motif for structure **X** is the finite 1–D $\{Sm_8O_{58}\}$ octamer extending in the [½ –1 ½] direction, as shown in Figure 6.14. Each octamer is made up of eight edge–shared pseudo–monocapped square anti–prisms arranged in the following sequence; Sm(4)···Sm(3)···Sm(2)···Sm(1)···Sm(1)···Sm(2)···Sm(3)···Sm(4). It may be noted that half of the 1–D octamer is related to the other half by $\bar{1}$ symmetry. The coalescence of any two contiguous pseudo–monocapped square anti–prismatic $\{Sm^{III}O_9\}$ motifs occurs not only *via* the common oxygen edges, *i.e.* O(2)–O(7) for Sm(1)···Sm(2), O(10)–O(14) for Sm(2)···Sm(3), and O(20)–O(22) for Sm(3)···Sm(4), but also the $\mu_2-\eta^1{:}\eta^1$ (*syn–syn*) carboxylato O atoms, *i.e.* O(8)–C(9)–O(9) for Sm(1)···Sm(2), O(12)–C(11)–O(17) and O(13)–C(16)–O(21) for Sm(2)···Sm(3), and O(19)–C(18)–O(23) for Sm(3)···Sm(4).

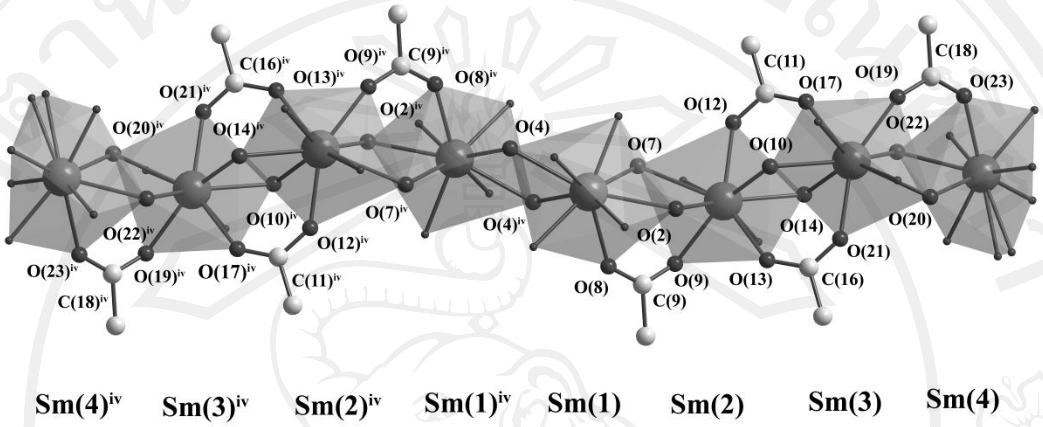

Figure 6.14 The {Sm_8O_{58}} octamer units in **X**. Symmetry code: (iv) [$x - 1, y, z$].

The 1–D {Sm_8O_{58}} octamers are connected to the adjacent segments in the [½ –1 ½] direction by the $\mu_2{-}\eta^1{:}\eta^1$ (*syn*–*anti*) carboxylate group as depicted in Figure 6.15. The infinite 1–D coordination chains of the {Sm_8O_{58}} segments are therefore established, and further connected in the crystal structure by the TTHA ligands to form a rather dense 3–D packing as shown in Figure 6.16. In addition, the auxiliary *L2* ligand which is also completely deprotonated adopts the $\mu_1{-}\eta^1{:}\eta^1$ mode of coordination and transfixes two adjacent Sm(4) ions in the direction of *a* as depicted in Figure 6.17. This is to form an auxiliary chain and increase the density of the framework. As it is revealed by the characteristic N–H absorption in the IR spectrum of **X** (Figure 6.18), the protonation at N atoms of the *L2* ligand can be assumed. This then neutralizes the negative charge on the dicarboxylato units of the ligand and therefore charge of the framework.

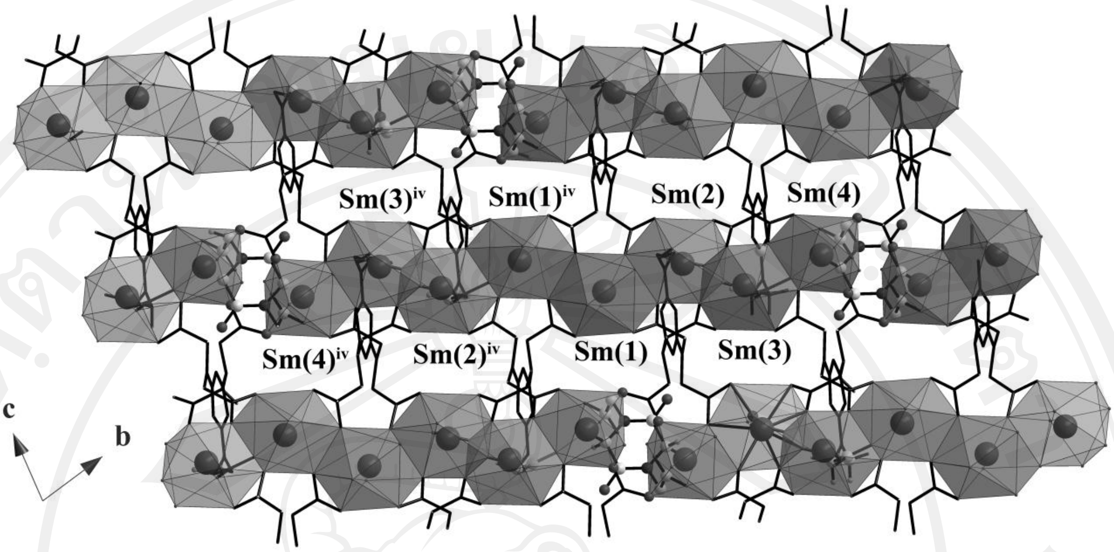

Figure 6.15 The 1–D {Sm_8O_{58}} octamers lying in the [½ −1 ½] direction. Water of crystallization and hydrogen atoms are omitted for clarity. Symmetry code: (iv) [$x - 1, y, z$].

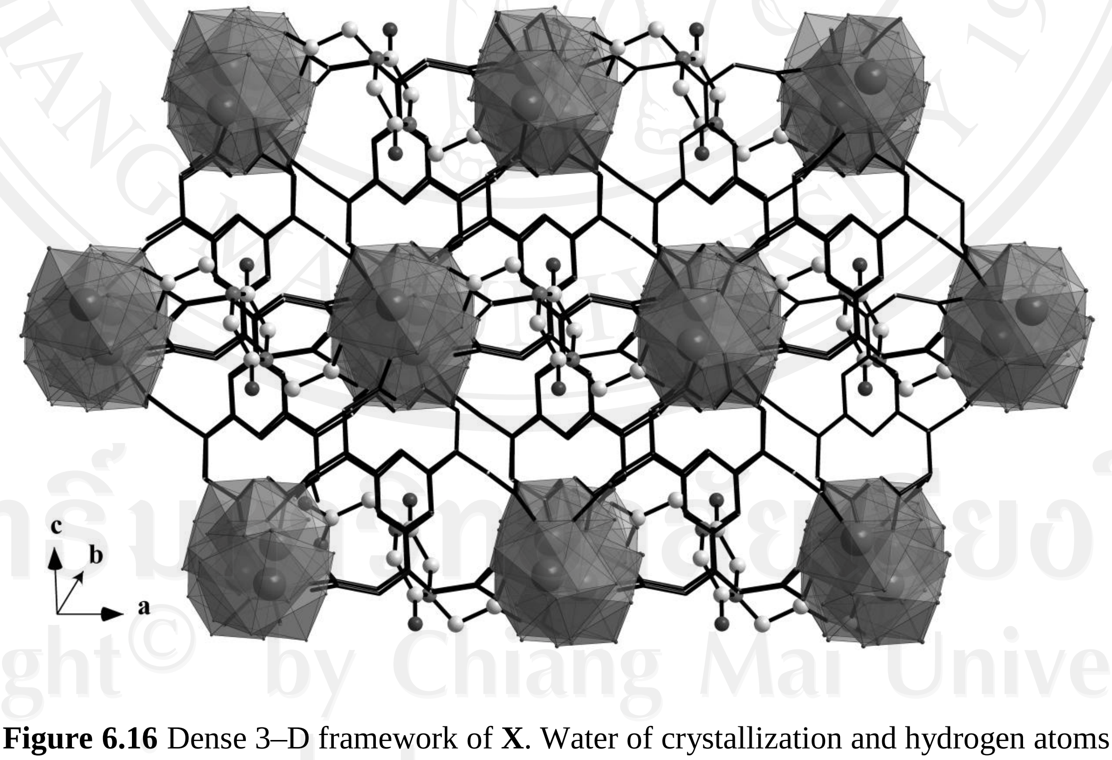

Figure 6.16 Dense 3–D framework of **X**. Water of crystallization and hydrogen atoms are omitted for clarity.

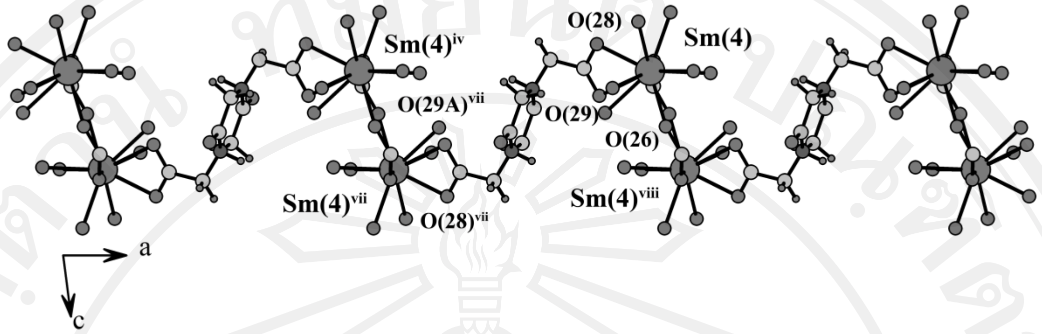

Figure 6.17. The 1−D chain of *L2* ligand and two adjacent Sm(4) ions in *a* direction.

Symmetry codes: (iv) [$x - 1, y, z$] (vii) [$-x + 1, -y, -z + 1$] (viii) [$-x + 2, -y, -z + 1$].

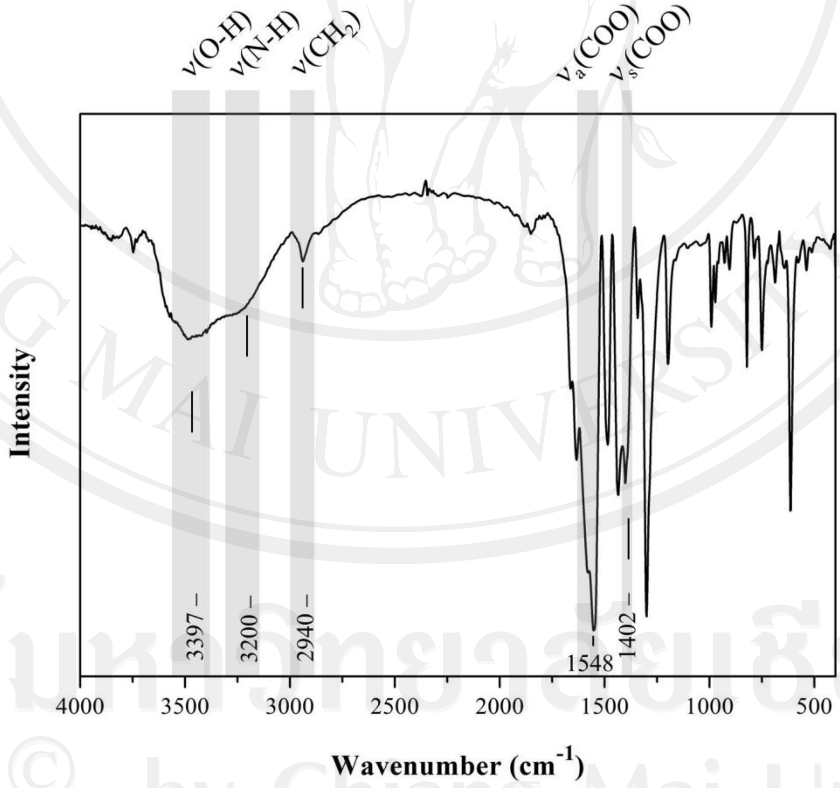

Figure 6.18 FT−IR spectrum of compound **X** with selected band indexing.

According to the calculation using PLATON [23], there are more free space in the framework of **X** (*ca.* 13.1%) in comparison to that of the isostructural **IXa** and **IXb** (*ca.* 5.3%). The crystallizing water molecules occupy the framework void, and apparently involve in both the O–H···O and C–H···O hydrogen bonding interactions as listed in Table 6.13.

Table 6.13 List of the hydrogen bonding interactions in **X**.

D – H ··· A [a]	D – H, (Å)	H ··· A, (Å)	D ··· A, (Å)	D – H ··· A, (°)
O(1W) ··· O(9)	–	–	2.845(8)	–
O(1W) ··· O(11)	–	–	2.922(8)	–
O(1W) ··· O(15)	–	–	2.705(7)	–
O(2W) ··· O(16)^{iv}	–	–	2.865(7)	–
O(2W) ··· O(18)^{ii}	–	–	2.893(7)	–
O(2W) ··· O(19)^{iv}	–	–	2.757(9)	–
C(2) – H(2A) ··· O(13)	0.97	2.51	3.337(13)	143
C(12) – H(12A) ··· O(3W)	0.97	2.41	3.349(17)	162
C(23) – H(23B) ··· O(28)	0.97	2.50	3.205(15)	130
C(32) – H(32B) ··· O(30)	0.97	2.20	2.63(3)	106
C(33) – H(33B) ··· O(29A)	0.97	2.58	3.09(3)	113

[a] Symmetry codes: (ii) [$-x + 1, -y + 1, -z + 1$] (iv) [$x - 1, y, z$].

6.2.3 Crystal structures of [$Ln_4(C_{15}H_{13}O_{12}N_6)_2(SO_4)(H_2O)_4$]·$4H_2O$, Ln = Pr^{III} (XIa) and Nd^{III} (XIb)

Using Nd^{III} and Pr^{III} as the target metal, two isostructural compounds [$Ln_4(C_{15}H_{13}O_{12}N_6)_2(SO_4)(H_2O)_4$]·$4H_2O$, where Ln = Pr^{III} (**XIa**) and Nd^{III} (**XIb**) have been synthesized under the same synthetic condition. Compounds **XIa** and **XIb** are distinct from the previous structures in that they present the sulfate anion as auxiliary diverging ligand and polycarboxylato ligand is not fully deprotonated. For the sake of consistency, the crystal structure of [$Pr_4(C_{15}H_{13}O_{12}N_6)_2(SO_4)(H_2O)_4$]·$4H_2O$ (**XIa**) will be representatively presented. The structure of **XIa** crystallizes in the triclinic $P\bar{1}$ space group with comparable unit cell parameters and volume to those of **IXa** and **IXb** (Table 6.2). The asymmetric unit of **XIa** consists of forty–two non–hydrogen atoms, including two distinct Pr^{III} ions, a whole molecule of H−TTHA, a sulfate anion and water molecules as depicted in Figure 6.19. There are two types of disorder displayed in this structure; (i) the site disorder of the whole sulfate and (ii) the substitutional disorder of the sulfate and the coordinated water molecule.

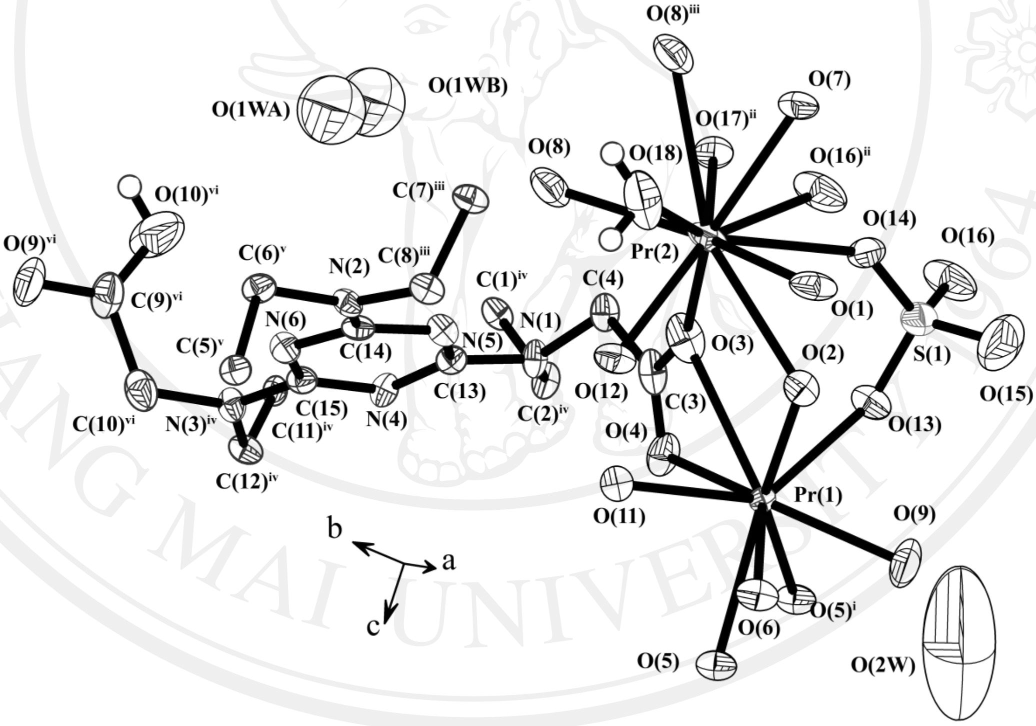

Figure 6.19 ORTEP presentation of the asymmetric unit of **XIa** with displacement ellipsoids (60% probability) and atomic labeling for non–hydrogen atoms. Hydrogen atoms are omitted for clarity. Symmetry codes: (i) [–*x*, –*y*, –*z* + 2] (ii) [–*x*, –*y*, –*z* + 1] (iii) [–*x*, –*y* + 1, –*z* + 1] (iv) [*x* – 1, *y*, *z*] (v) [–*x*, –*y* + 1, –*z* + 2] (vi) [*x* – 1, *y* + 1, *z*].

Figure 6.20 depicts the nine–fold coordination environments of different geometries adopted by Pr(1) and Pr(2). The coordination sphere about Pr(1) is pseudo–tricapped trigonal prismatic in shape, delineated by eight O atoms from five H–TTHA molecules and one O atom (O(13)) from either the sulfate anion or the water molecule due to the half sharing of site occupancy for the two motifs. The Pr(2) ions shows rather complicated coordination environment according to the existing disorder. The substitional disorder suggest the alternative presence of either the sulfate (O(14) or O(16)) or the ligated water (O(17)). The concurrent presence of both structural motifs at the same whereabouts is chemically impracticable. If the sulfate is present, the surrounding of Pr(2) will be outlined by seven O atoms from three H–TTHA, one O atom from water molecule (O(18)), and the disordering O(14) and O(16) of the sulfate. This then makes the coordination about the Pr(2) ion to be the nine–fold distorted polyhedra. If the water molecule (O(17)) is taken into account instead of the sulfate, then the coordination of Pr(2) will include two ligated water molecules and the coordination geometry will be also the nine–fold polyhedra. Regarding the disorder of the sulfate anion, it is allocated between two site related by the $\bar{1}$ operation as depicted in Figure 6.21. The sulfate therefore function as an auxiliary diverging ligand bridging the neighboring Pr(1) and Pr(2) using O(13) and O(14) or O(16).

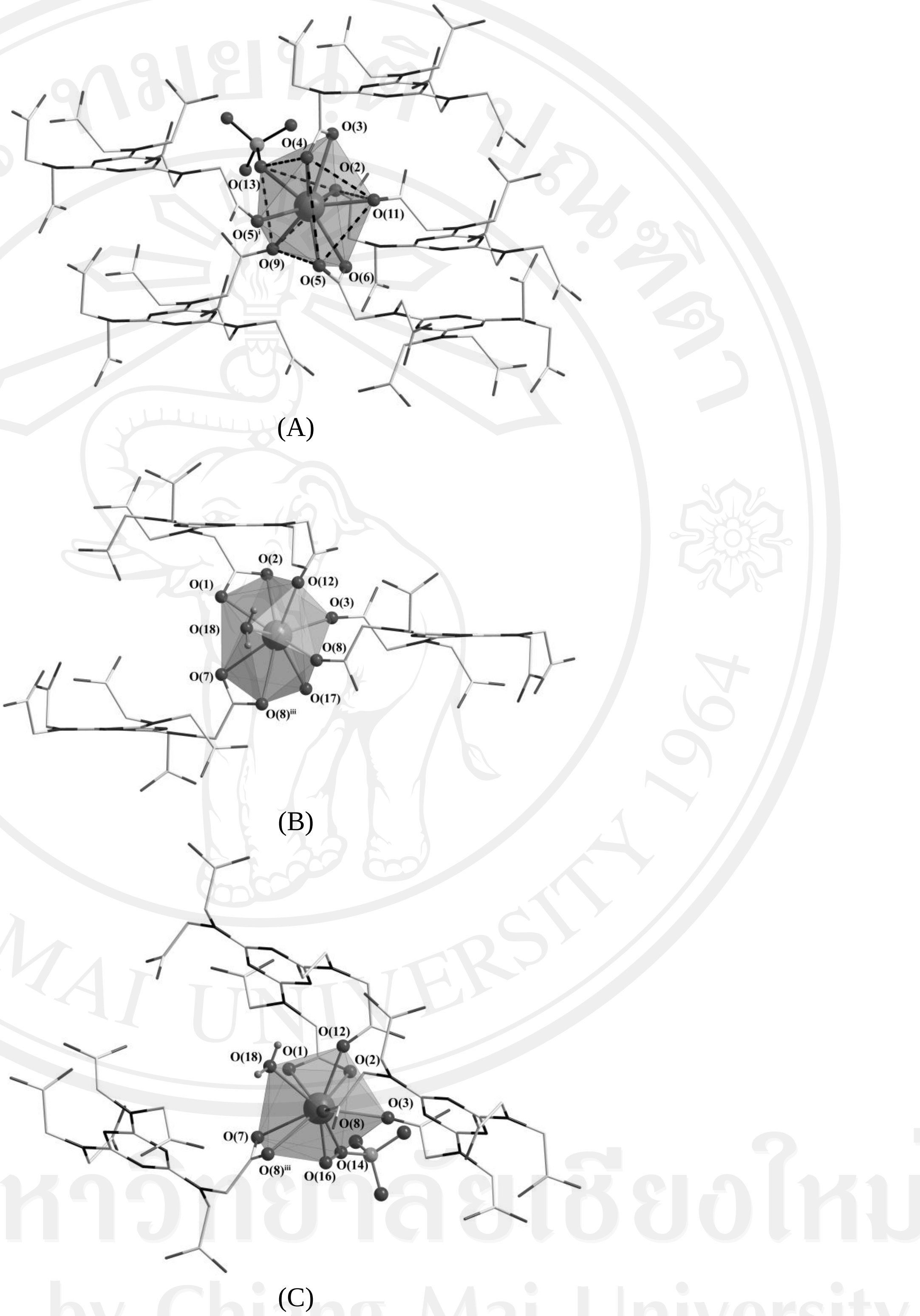

Figure 6.20 View of the Pr^{III} and the surrounding TTHA ligands. (A) Pr(1) (B) Pr(2) with O(17) and (C) Pr(2) with O(14) and O(16) as a ligand. Symmetry codes: (i) [–*x*, –*y*, –*z* + 2] (iii) [–*x*, –*y* + 1, –*z* + 1].

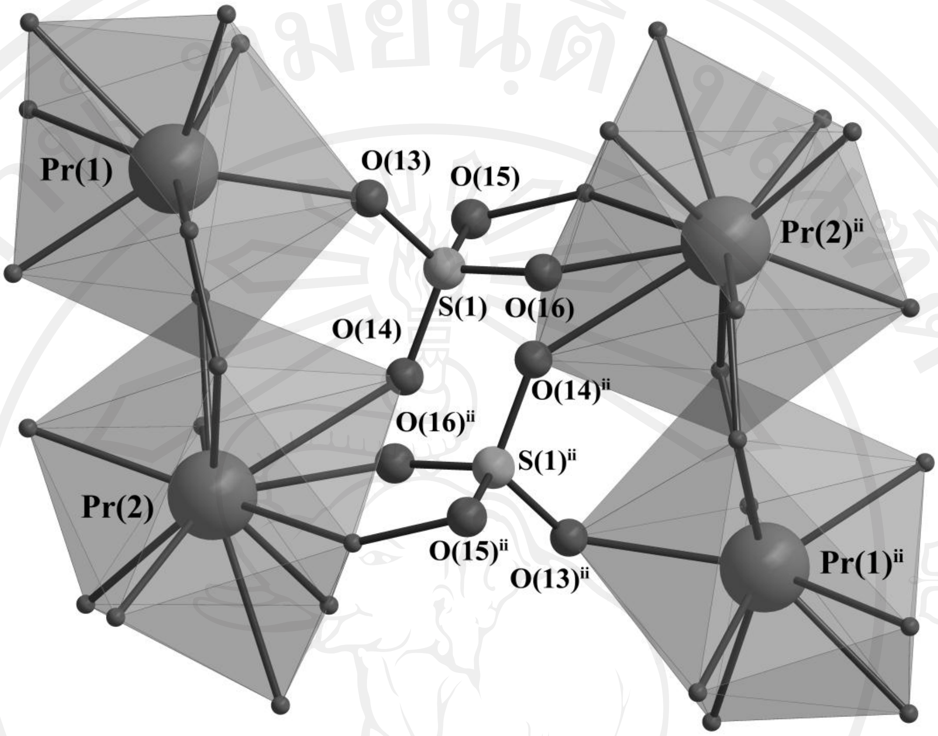

Figure 6.21 The disorder of the sulfate anion. Symmetry codes: (ii) [–*x*, –*y*, –*z* + 1].

Considering the Ln : H–TTHA : water/sulfate, compounds **XIa** and **XIb** exhibit unprecedentedly high ratio of 1 : 5 : 1 in the case of Pr(1). The Ln : H–TTHA : water/sulfate ratio for Pr(2) is 1 : 3 : 2.

In a similar fashion to **IXa** and **IXb** frameworks, two pseudo–tricapped trigonal prismatic {Pr(1)O_9} are fused through a common edge generated from the carboxylato O(5) atom to from {Pr(1)$_2O_{16}$} dimer whereas a couple of distorted polydra {Pr(2)O_9} is combined to form the other {Pr(2)$_2O_{16}$} dimer by sharing edge generated from O(8) of also the carboxylate. These dimers are then alternatively condensed using the common O(2)–O(3) edge, the carboxylato O(12)–C(11)–O(11) and the sulfate O(14)–S(1)–O(13) to form the infinite 1–D chain in the direction of [0

–½ ½] as shown in Figure 6.22. The extended infinite 1–D chains and the stacking of them are depicted in Figure 6.23. As revealed in Figure 6.24, the disordering sulfate anions also link the {Pr(1)O_9} and the {Pr(2)O_9} motifs to form another infinite 1–D chain in the direction of *b*. Due to the disorder at the sulfate, two bridging modes including 2.1100 and 3.1110 are feasible.

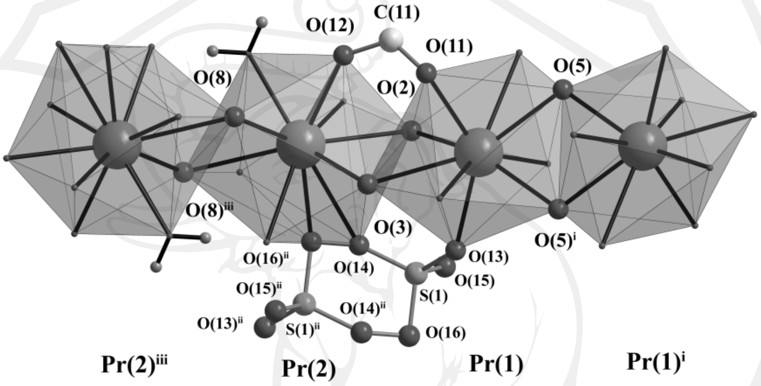

Figure 6.22 The structural building dimers; {Pr(1)$_2$O$_{16}$} and {Pr(2)$_2$O$_{16}$}. Symmetry codes: (i) [–*x*, –*y*, –*z* + 2] (ii) [–*x*, –*y*, –*z* + 1] (iii) [–*x*, –*y* + 1, –*z* + 1].

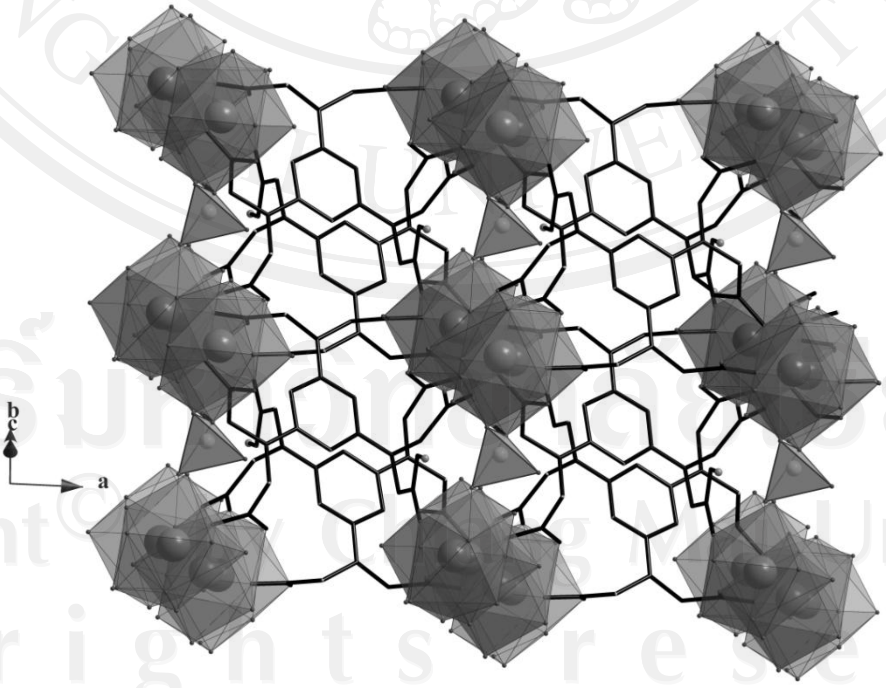

Figure 6.23 The condensation of 1–D chains viewed along [0 –½ ½] axis.

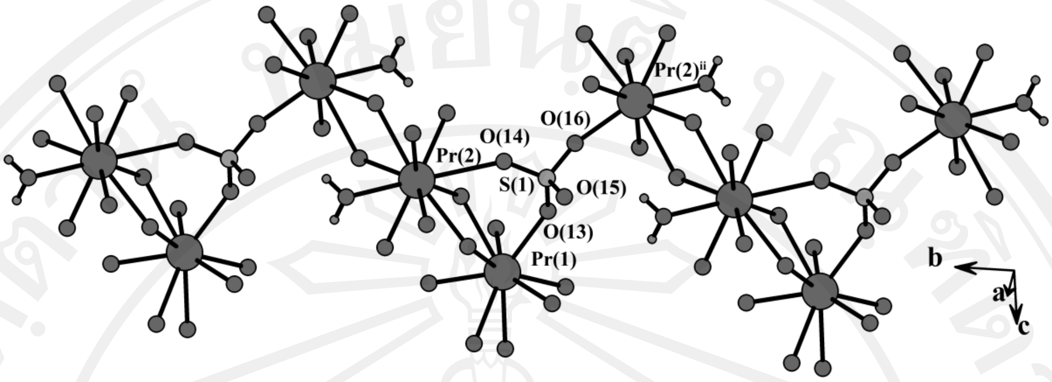

Figure 6.24 The 3.1110 bridging mode of the sulfate anion linking the $\{Pr(1)O_9\}$ and $\{Pr(2)O_9\}$ motifs of 1–D chain along [0 –½ ½] and the $\{Pr(2)O_9\}$ with the adjacent $\{Pr(2)O_9\}$ along the *b* direction. Symmetry codes: (ii) [–*x*, –*y*, –*z* + 1].

The H–TTHA ligands present in the structure of **XIa** and **XIb** exhibit three different modes of coordination as detailed in Table 6.11, including $\mu_2-\eta^2:\eta^1$, $\mu_2-\eta^1:\eta^1$ (*syn–syn*) and $\mu_1-\eta^1:\eta^0$, the latest of which does not found in the other related frameworks. Each H–TTHA adopts the accumulative $\mu_8-\eta^{15}$ mode of coordination in assembling the neighboring five Pr(1) and three Pr(2) together as depicted in Figure 6.25. Concerning the conformation of the dicarboxylato arms of the H–TTHA ligand, there exists the *cis* conformation in addition to the commonly found *trans* arrangement for a pair of the dicarboxylato arms docked to the same N atom.

The framework structure of **XIa** is nano–porous in nature, possesses a void volume of 11.0 % calculated using PLATON [23]. The void structure is 1–D channel extending in the direction of *b* and, is apparently occupied by water of crystallization as shown in Figure 6.26. The strong hydrogen–bond interactions of O–H···O type are found between the protonated O atom of the HTTHA and O atoms of both the coordinated and the crystallized water. Moreover weak hydrogen bond interactions (C–H···O) are also established involving the HTTHA as listed in Table 6.14.

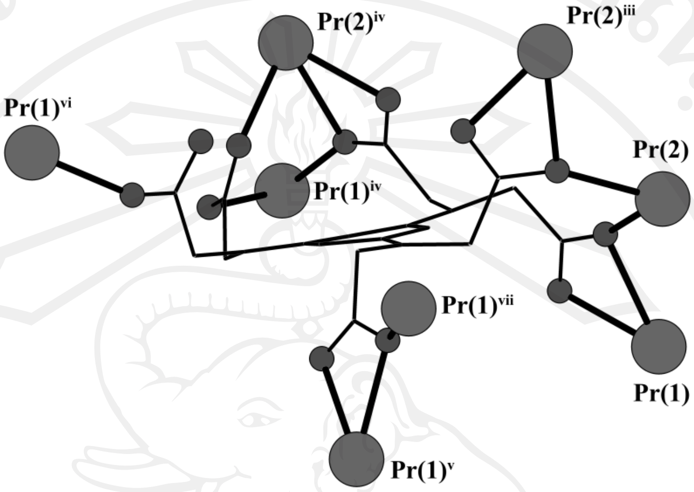

Figure 6.25 The assembly of five Pr(1) and three Pr(2) about the TTHA ligand in **XIa**. Symmetry codes: (iii) [–*x*, –*y* + 1, –*z* + 1] (iv) [*x* – 1, *y*, *z*] (v) [–*x*, –*y* + 1, –*z* + 2] (vi) [*x* – 1, *y* + 1, *z*] (vii) [*x*, *y* + 1, *z*].

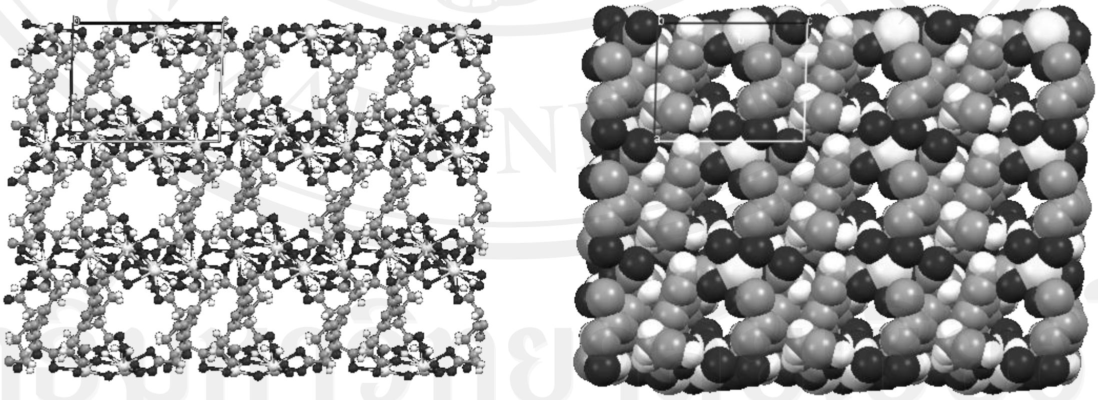

Figure 6.26 Circular channels extending along *b* axis in **XIa**.

Table 6.14 List of the hydrogen bonding interactions and geometries in **XIa**.

D – H ··· A ^{a}	D – H, (Å)	H ··· A, (Å)	D ··· A, (Å)	D – H ··· A, (°)
O(1WA) ··· O(7)^{iii}	–	–	2.7882(3)	–
O(1WB) ··· O(7)^{iii}	–	–	2.8767(3)	–
O(2W) ··· O(6)^{viii}	–	–	2.6668(2)	–
O(2W) ··· O(9)	–	–	2.9982(3)	–
O(10) – H(10) ··· O(13)	0.82	2.42	3.090(9)	139
O(10) –H(10) ··· O(15)	0.82	1.87	2.630(15)	153
O(18) –H(18A) ··· O(10)^{vii}	0.85(4)	2.05(5)	2.811(9)	149(6)
O(18) –H(18B) ··· O(17)^{vii}	0.83(5)	1.85(6)	2.609(11)	152(6)
C(2) – H(2A) ··· O(6)	0.97	2.47	3.353(6)	151
C(6) – H(6B) ··· O(2W)^{viii}	0.97	2.38	3.11(7)	131
C(6) – H(6B) ··· N(6)^{v}	0.97	2.43	2.797(7)	102
C(10) – H(10A) ··· O(2W)	0.97	2.24	3.05(7)	140
C(10) – H(10B) ··· O(4)^{i}	0.97	2.49	3.254(7)	135
C(12) – H(12B) ··· O(6)	0.97	2.50	3.262(6)	135

^{a} Symmetry codes: (i) [–*x*, –*y*, –*z* + 2] (iii) [–*x*, –*y* + 1, –*z* + 1] (v) [–*x*, –*y* + 1, –*z* + 2] (vii) [x, y + 1, z] (viii) [-x + 1, -y, -z + 2].

6.2.4 Crystal structure of $[Sm_2(C_{15}H_{12}O_{12}N_6)(H_2O)_4]\cdot 9H_2O$ (XII)

The last structure reported here is the open framework structure of $[Sm_2(C_{15}H_{12}O_{12}N_6)(H_2O)_4]\cdot 9H_2O$ (**XII**), which add to a series of isostructural compounds with general formula $[Ln^{III}{}_2(C_{15}H_{12}O_{12}N_6)(H_2O)_4]\cdot 9H_2O$ where Ln^{III} = Eu^{III}, Gd^{III}, Tb^{III} and Dy^{III}, previously reported by Q. Zhu *et.al.* in 2009 [12]. Apparently, Sm^{III} with electronic configuration $[Xe]4f^{5}$ precedes Eu^{III} ($[Xe]4f^{6}$), Gd^{III} ($[Xe]4f^{7}$), Tb^{III} ($[Xe]4f^{8}$) and Dy^{III} ($[Xe]4f^{9}$) in the lanthanide series. The framework structure of **XII** significantly differs from the other titled frameworks in that the framework crystallizes in the monoclinic space group *C*2/*c* rather than the triclinic $P\bar{1}$ (Table 6.2), and is vividly open with well organized channel structure.

The asymmetric unit of **XII** includes only one Sm^{III} ion, half of the completely deprotonated TTHA, and water of crystallization as shown in Figure 6.27. The Sm^{III} ion adopts the common nine–fold coordination of pseudo–monocapped square anti–prismatic geometry, which is characterized by seven O atoms from three TTHA and two ligated water O atoms (O(7) and O(8)). The two water O atoms are notably located adjacent to each other as depicted in Figure 6.28. The $\{Sm^{III}O_9\}$ motifs are further condensed to form a $\{Sm^{III}_2O_{18}\}$ dimer by sharing edge which involves two carboxylato O(4) atoms and two $\mu_2-\eta^1:\eta^1$ carboxylato ligand (O(6)–C(5)–O(5)) related by $\bar{1}$ symmetry. The four coordinated water molecules are notably located on the far opposite edges of the dimer. Each dimer is present as an isolated building motif and is surrounded by four TTHA ligands as shown in Figure 6.28, which makes the Sm^{III} : TTHA : water ratio to be 1 : 2 : 1. The four TTHA ligands in the neighborhood of the $\{Sm^{III}_2O_{18}\}$ dimer then connect the dimer to as many as ten other encompassing dimers from which the 3–D framework is fabricated as depicted in Figure 6.29. In comparison to the frameworks of **IXa** (**IXb**), **X** and **XIa** (**XIb**), the presence of the isolated building motif, *i.e.* the $\{Sm^{III}_2O_{18}\}$ dimer, in **XII** rather than the 1–D segment or chain accounts for the apparently more open framework in **XII**.

The TTHA ligand in structure **XII** displays three modes of coordination, *i.e.* $\mu_2-\eta^2:\eta^1$, $\mu_2-\eta^1:\eta^1$ (*syn–syn*), which are common to the other titled frameworks, and $\mu_1-\eta^1:\eta^1$ which is distinct. The cumulative mode of coordination for the TTHA is $\mu_6-\eta^{14}$ binding six surround $\{Sm^{III}O_9\}$ motifs from four $\{Sm^{III}_2O_{18}\}$ dimers as shown in Figure 6.30. The commonly found *trans* conformation is also adopted by the dicarboxylato arms anchored onto the same N atom of the TTHA.

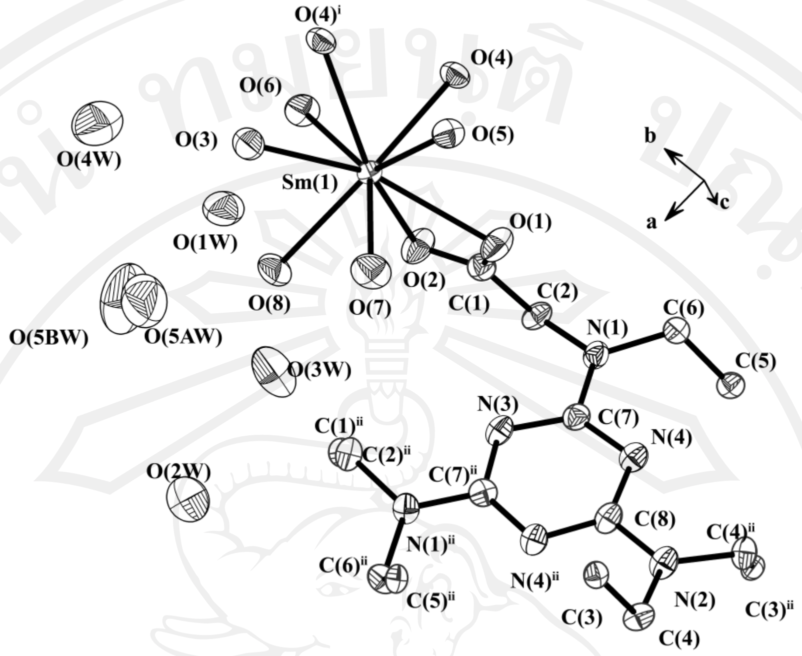

Figure 6.27 View of the extended asymmetric unit of **XII** and the pseudo–monocapped square anti–prismatic geometry of Sm(1)^{III} with displacement ellipsoids (70% probability) and atomic labeling for non–hydrogen atoms. Hydrogen atoms are omitted for clarity. Symmetry codes: (i) [–*x* + 0.5, –*y* + 0.5,–*z*] (ii) [–*x* + 1, *y*, –*z*+0.5].

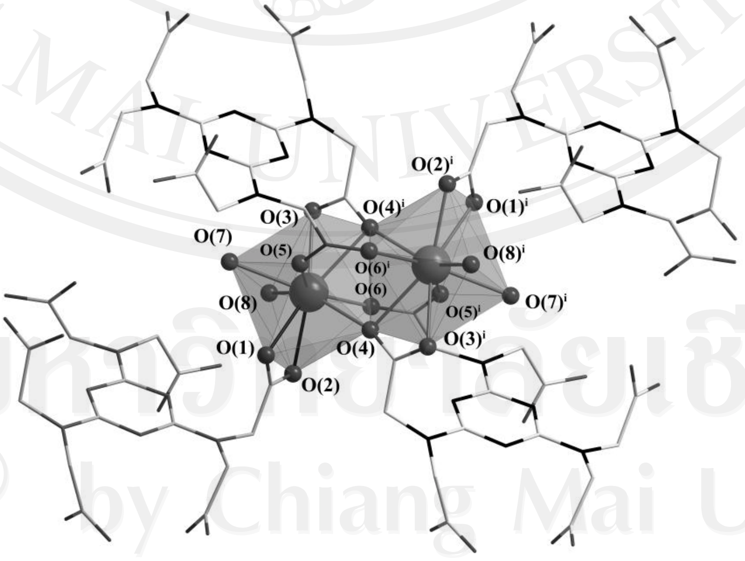

Figure 6.28 View of the $\{\mathrm{Sm^{III}_2O_{18}}\}$ dimer and the surrounding TTHA ligands. Symmetry codes: (i) [–*x* + 0.5, –*y* + 0.5,–*z*].

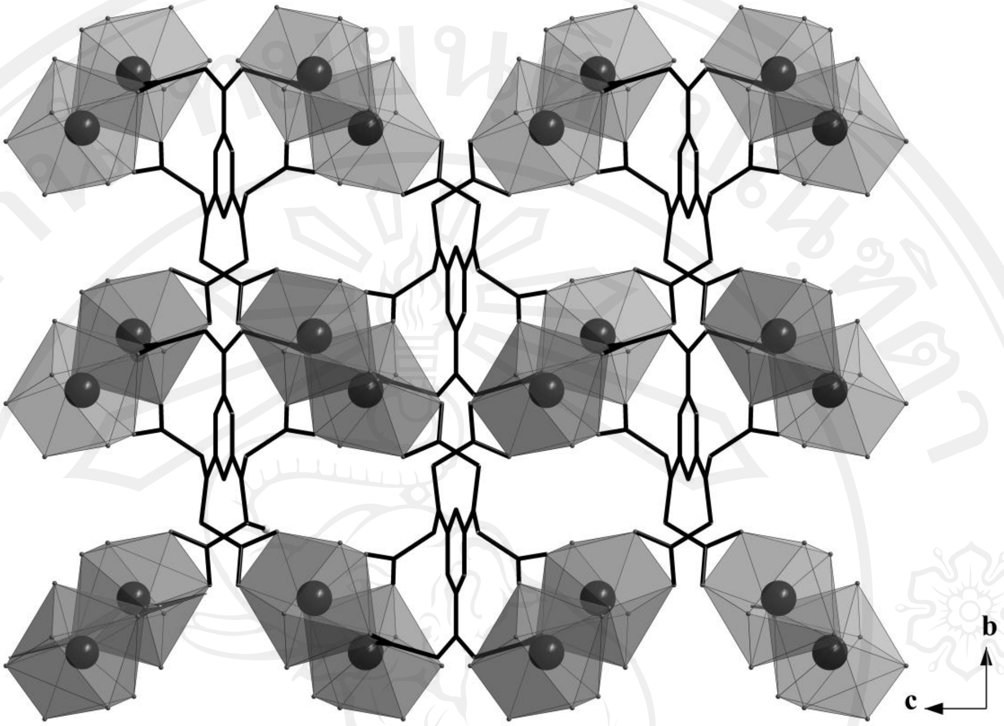

Figure 6.29 Arrangement of $\{Sm^{III}{}_2O_{18}\}$ dimer viewed along *a* direction.

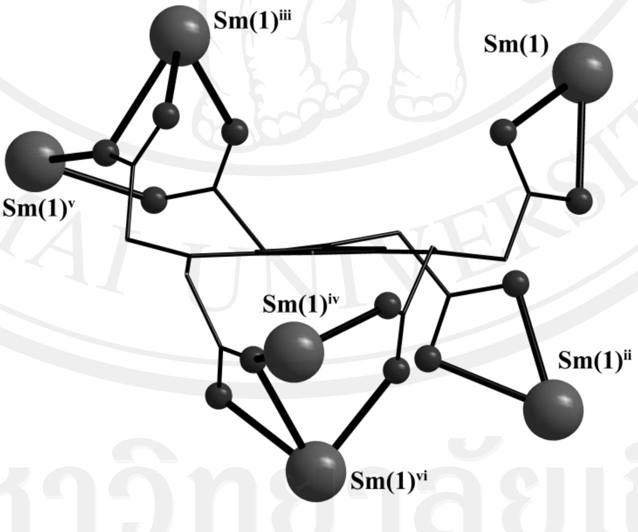

Figure 6.30 The assembly of six Sm(1) about the TTHA ligand in **XII**. Symmetry codes: (ii) [–*x* + 1, *y*, –*z*+0.5] (iii) [–*x* + 1, –*y*, –*z*] (iv) [–*x* + 0.5, *y* + 0.5, –*z* + 0.5] (v) [*x* + 0.5, *y* – 0.5, *z*] (vi) [*x*, –*y*, *z* + 0.5].

The framework structure of **XII** can be viewed as composing of 3–D channels which extend in two different directions arranged at right angle as illustrated in Figure 6.31. The large elliptical channels of effective dimensions 9.05 Å × 4.11 Å based on the closest opposite O atoms (O(6) and O(3)) stretch in the [1 1 0] direction. The smaller circular channels of effective diameter 4.57 Å based on the distance between the opposite O(6) atoms, lie along the direction of *c* axis and intersect with the large channel. According to the calculation provided in PLATON [23], the total void volume is 31.6% (994.7 $Å^3$). Within the void gallery, the water of crystallization is housed. In comparison to the previous report on a series of isostructural $[Ln_2(C_{15}H_{12}O_{12}N_6)(H_2O)_4]\cdot 9H_2O$ [12], The calculated channel dimensions and free space in the framework of **XII** are only slightly smaller, which should be due to the larger ionic radii for Sm^{III}. The classical hydrogen bond interaction is not found in this compound because no hydrogen atoms could be located with accuracy on the water molecules. However this interaction can be estimated based on the distances between donor and accepter atoms as detailed in Table 6.15.

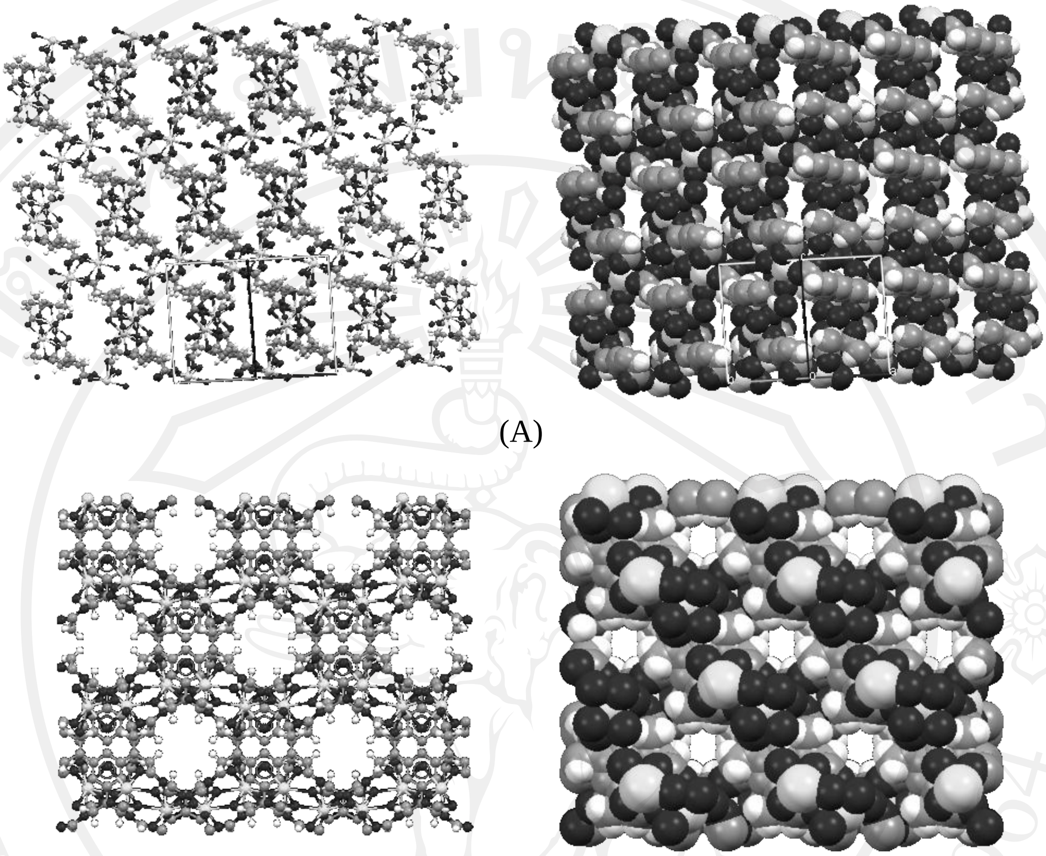

(A)

(B)

Figure 6.31 (A) Elliptical channels lying along [1 1 0] direction and (B) Circular channels lying along *c* direction.

Table 6.15 List of the hydrogen bonding interactions and geometries in **XII**.

D – H ··· A [a]	D – H, (Å)	H ··· A, (Å)	D ··· A, (Å)	D – H ··· A, (°)
O(1W) ··· O(4W)	–	–	2.7743(84)	–
O(2W) ··· O(3W)	–	–	2.8260(84)	–
O(2W) ··· O(4W)^{vii}	–	–	2.7184(93)	–
O(3W) ··· O(5AW)	–	–	2.5445(21)	–
O(3W) ··· O(5BW)	–	–	2.9801(18)	–
O(7) ··· O(3W)	–	–	2.7195(73)	–
O(8) ··· O(5AW) #2	–	–	2.8102(18)	–
O(8) ··· O(5BW) #2	–	–	2.6903(22)	–

[a] Symmetry codes: (vii) [x + 0.5, y – 0.5, z] (ix) [-x + 1.5, -y + 0.5, -z].

6.3 Conclusions

Six new lanthanide frameworks with a flexible TTHA ligand were successfully synthesized by carefully adjusting the hydrothermal reaction time (72 h 48 h) and the Ln:H_6TTHA mole ratios, *i.e.* Ln:H_6TTHA = 2:1.6, and 2:1. The crystal structures can be divided in to four distinct structures; $Ln_4(C_{15}H_{12}O_{12}N_6)_2(C_8H_{10}O_6N_2)_{0.5}(H_2O)_3.5H_2O$ (Ln = Pr^{III} **(IXa)** and Nd^{III} (**IXb)**) $Sm_8(C_{15}H_{12}O_{12}N_6)_4(C_8H_8O_6N_2)_{0.5}(H_2O)_8.4H_2O$ **(X)**, $Ln_4(C_{15}H_{13}O_{12}N_6)_2(SO_4)(H_2O)_4.2H_2O$ (Ln = Pr^{III} (**XIa**) and Nd^{III} (**XIb**)) and $Sm_2(C_{15}H_{12}O_{12}N_6)(H_2O)_4.9H_2O$ **(XII)**. The prolongation of the hydrothermal reaction time apparently led to the decomposition of the H_6TTHA molecules to a smaller dicarboxylate ligand; 2,5–dioxo–piperazine–1,4–diacetic acid which acts as an auxiliary ligand in the frameworks **IXa**, **IXb** and **X**. The control of Ln:H_6TTHA ratio results in a different structural arrangement. It is also apparent that the use of Pr^{III} and Nd^{III} leads to isostructure frameworks whereas Sm^{III} gives different results.

REFERENCES

1. R.J. Kuppler, D.J. Timmons, Q.–R. Fang, J.–R. Li, T.A. Makal, M.D. Young, D.Yuan, D. Zhao,W. Zhuang, H.-C. Zhou, Coord. Chem. Rev. 253 (2009) 3042.
2. J.D. Lin, X.F. Long, P. Lin, S.W. Du, Cryst. Growth Des. 10 (2010) 146.
3. K.S. Murray, C.J. Kepert, Cooperativity in Spin Crossover Systems: Memory, Magnetism and Microporosity, Springer–Verlag, 2004.
4. M.D. Allendorf, C.A. Bauer, R.K. Bhakta, R.J.T. Houk, Chem. Soc. Rev. 38 (2009) 1330.
5. Y. Hasegawa, Y. Wada, S. Yanagida, J. Photochem. Photobiol. C: Photochem. Rev. 5 (2004) 183.
6. B.D. Chandler, D.T. Cramb, G.K.H. Shimizu , J. Am. Chem. Soc. 128 (2006) 10403.
7. D. Imbert, N.F. Rouge, J.-C.G. Bünzli, Eur. J. Inorg. Chem. (2003) 1332.
8. S.-N. Wang, J. Bai, Y.-Z. Li, Y. Pan, M. Scheer, X.-Z. You, Cryst. Eng. Comm. 9 (2007) 1084.
9. S.-N. Wang, R. Sun, X.-S. Wang, Y.-Z. Li, Y. Pan, J. Bai, M. Scheer, X.-Z. You, Cryst. Eng. Comm. 9 (2007) 1051.
10. Q. Zhu, T. Sheng, R. Fu, S. Hu, J. Chen, S. Xiang, C. Shen, X. Wu, Cryst. Growth Des. 9 (2009) 5128.
11. Cambridge Structural Database Version 5.33 (update May 2012). Cambridge Crystallographic Data Centre, 12 Union Road, Cambridge, England, 2012.
12. Q. Zhu, T. Sheng, R. Fu, S. Hu, J. Chen, S. Xiang, C. Shen, X. Wu, Cryst. Growth Des. 9 (2009) 5128.

13. W. Karuehanon, W. Fanfuenha, A. Rujiwatra, M. Pattarawarapan, Tetrahedron Lett. 53 (2012) 3486.
14. J. de Meulener, H. Tompa, Acta Crystallogr. 19 (1965) 1014.
15. G.M. Sheldrick (1997) SHELXS−97, program for solving crystal structure. University of Gottingen, Germany.
16. G.M. Sheldrick (1997) SHELXL−97, program for crystal structure refinement. University of Gottingen, Germany
17. L.J. Farrugia, J. Appl. Crystallogr. 32 (1999) 837.
18. V.S. Urusov, I.P. Orlov, Crystallogr. Rep. 44 (1999) 686.
19. X.−J. Kong, G.−L. Zhuang, Y.−P. Ren, L.−S. Long, R.−B. Huang, L.−S. Zheng, Dalton Trans. (2009) 1707.
20. P. Müller, R.H. Irmer, A.L. Spek, T.R. Schneider, M.R. Sawaya, Crystal Structure Refinement: A Crystallographer’s Guide to SHELXL, Oxford University Press Inc., New York, 2006.
21. H.A. Ankersmit, P.T. Witte, H. Kooijman, M.T. Lakin, A.L. Spek, K. Goubitz, K. Vrieze, G. Koten. Inorg. Chem. 35 (1996) 6053.
22. G. Albertin, S. Antoniutti, A. Bacchi, E. Bordignon, F. Miani, G. Pelizzi, Inorg. Chem. 29 (2000) 3283.
23. A. L. Spek, (2002) PLATON, University of Utrecht, The Netherlands.